

Review

Methane Reforming Processes: Advances on Mono- and Bimetallic Ni-Based Catalysts Supported on Mg-Al Mixed Oxides

Soroosh Saeedi ^{1,2,†}, Xuan Trung Nguyen ^{1,2,†} , Filippo Bossola ¹, Claudio Evangelisti ^{3,*} 
and Vladimiro Dal Santo ^{1,*} ¹ CNR-Istituto di Scienze e Tecnologie Chimiche “Giulio Natta” (SCITEC), Via Golgi 19, 20133 Milano, Italy² Dipartimento di Scienza e Alta Tecnologia, Università degli Studi dell’Insubria, Via Valleggio 11, 22100 Como, Italy³ CNR-Istituto di Chimica dei Composti Organometallici (ICCOM), Via G. Moruzzi 1, 56124 Pisa, Italy

* Correspondence: claudio.evangelisti@cnr.it (C.E.); vladimiro.dalsanto@cnr.it (V.D.S.)

† These authors contributed equally to this work.

Abstract: Ni-based catalysts supported on Mg-Al mixed oxides (Mg(Al)O) have been intensively investigated as catalysts for CH₄ reforming processes (i.e., steam reforming (SMR) and dry reforming (DRM)), which are pivotal actors in the expanding H₂ economy. In this review, we provide for the first time an in-depth analysis of homo- and bimetallic Ni-based catalysts supported on Mg(Al)O supports reported to date in the literature and used for SMR and DRM processes. Particular attention is devoted to the role of the synthesis protocols on the structural and morphological properties of the final catalytic materials, which are directly related to their catalytic performance. It turns out that the addition of a small amount of a second metal to Ni (bimetallic catalysts), in some cases, is the most practicable way to improve the catalyst durability. In addition, besides more conventional approaches (i.e., impregnation and co-precipitation), other innovative synthesis methods (e.g., sol-gel, atomic layer deposition, redox reactions) and pretreatments (e.g., plasma-based treatments) have shown relevant improvements in identifying and controlling the interaction among the constituents most useful to improve the overall H₂ productivity.

Keywords: hydrogen; steam reforming; nickel catalysts; magnesium aluminum mixed oxide



Citation: Saeedi, S.; Nguyen, X.T.; Bossola, F.; Evangelisti, C.; Dal Santo, V. Methane Reforming Processes: Advances on Mono- and Bimetallic Ni-Based Catalysts Supported on Mg-Al Mixed Oxides. *Catalysts* **2023**, *13*, 379. <https://doi.org/10.3390/catal13020379>

Academic Editors: Eugenio Meloni, Marco Martino and Concetta Ruocco

Received: 22 December 2022

Revised: 1 February 2023

Accepted: 2 February 2023

Published: 9 February 2023



Copyright: © 2023 by the authors. Licensee MDPI, Basel, Switzerland. This article is an open access article distributed under the terms and conditions of the Creative Commons Attribution (CC BY) license (<https://creativecommons.org/licenses/by/4.0/>).

1. Introduction

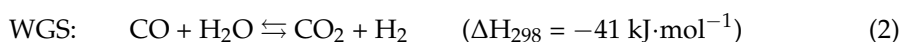
The rapid expansion of the H₂ economy, which has recently received new momentum from institutions such as the European Union with dedicated initiatives [1], calls for mid-term strategies to cope with the surge in demand. In this scenario, the conversion of CH₄ and/or biogas via thermo-catalytic reforming processes, that is, steam (SMR) and dry reforming (DRM), represents a solid strategy. The former is one of the best-established H₂ production technologies, which today accounts for most of the world’s production, while the latter allows the simultaneous conversion of two potent greenhouse gases into a valuable building block—the syngas, a mixture of CO and H₂ [2–6].

Since they are among the most used catalysts, several works have been dedicated to reviewing Ni-based catalysts for both reactions but are either focused on one reaction at a time and/or include the most different catalysts’ compositions [2–7]. Here we focused our attention on Ni catalysts supported on Mg-Al mixed oxides and modified with other metals. The reason is that, more than other catalysts, these Ni(M)/Mg(Al)O catalysts offer a unique opportunity to develop new strategies to address the many challenges posed by both SMR and DRM processes since both the synthetic protocol and/or the specific composition have a dramatic influence on the final catalytic activity. After a brief introduction recalling the main aspects of both reactions with a special emphasis on the role of the metal support

interaction, the impact of several preparation methods on the structure and catalytic activity of monometallic Ni catalysts will be discussed in detail, followed by a section describing the influence of other metals, i.e., bimetallic catalysts. Considering the sheer mole of data here reviewed and listed in tables that might render reading difficult, the main findings are summarized also in a schematic way in the final paragraph. In the hope of providing a useful guide for the development of future Ni-based catalysts for SMR and DRM reactions, we then singled out the most promising strategies along with some underestimated and/or unexplored pathways for improving the catalytic activity.

1.1. Steam and Dry Reforming Reactions of CH₄: General Aspects

In the CH₄-H₂O system, under the conditions of the steam reforming process, several chemical reactions are realized, of which the main ones are the steam reforming reaction (Equation (1)), which is strongly endothermic, and the water gas shift (WGS) reaction (Equation (2)), which is exothermic:



In this process (Equations (1) and (2)), four moles of H₂ are produced from each mole of methane, so that a large amount of H₂ can be obtained on an industrial scale [7,8]. Figure 1A shows the equilibrium conversion curve of SMR calculated by Joensen and Rostrup-Nielsen [9]. To achieve a high methane conversion, the reforming process should be carried out at a high temperature, low pressure, and a relatively high steam-to-methane molar ratio (3:1). Though SMR is a mature technology to produce H₂, the high energy required, the water consumption, and the use of methane with low-sulfur content are the main disadvantages of this process. Other critical issues are the simultaneous production of CO₂, which should be captured to avoid its emission into the environment, and the high cost of the overall process, which is still expensive compared to the US Department of Energy (DOE) cost of producing H₂ for future cars and other applications [10–12].

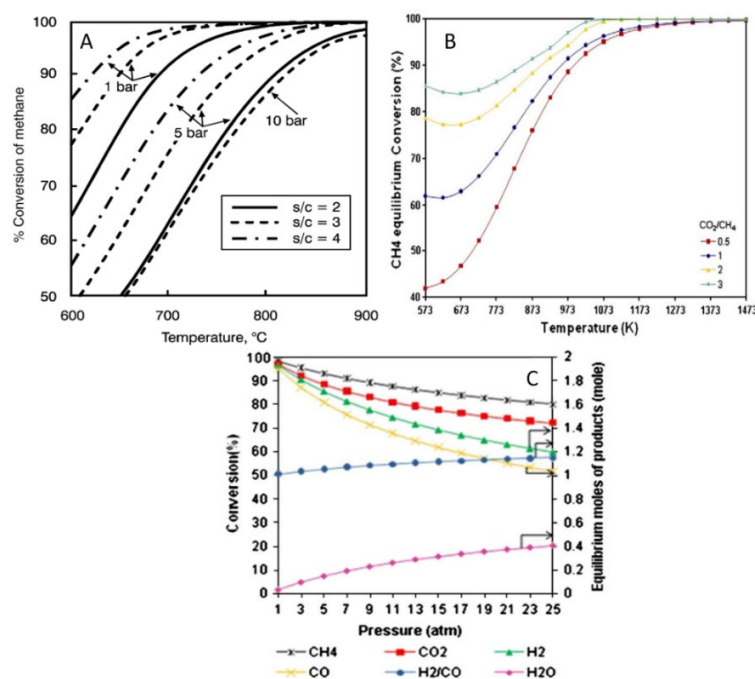


Figure 1. Equilibrium conversion of (A) SMR against temperature, pressure, and steam/methane ratio. Reprinted with permission from [9], copyright 2022, Elsevier. (B) DRM against temperature and CO₂/CH₄ ratio (C) DMR against reactants and products distribution for CO₂/CH₄ = 1, 900 °C and n(CH₄ + CO₂) = 2 mol. Reprinted with permission from [13], copyright 2011, Elsevier.

Like SMR, the DRM process is highly endothermic and as such is favored at high temperatures (700–900 °C). As CO₂ is one of the reactants, this type of methane reforming theoretically does not require any downstream CO₂ capture, which is a major perk. Moreover, the H₂/CO molar ratio of the produced syngas is typically around 1, which is lower than that of SMR and is particularly suited for the Fischer–Tropsch process [14,15]. The thermodynamics and equilibrium characteristics of DRM are the following:



The reverse water gas shift reaction (RWGS) occurs concurrently with DRM and, according to the studies of Bradford and Vannice, has a lower activation energy compared to H₂ formation [16]. In accordance with the equilibrium conversion curve of DRM (Figure 1B), CH₄ conversion increases rapidly below 727 °C and is generally favored at high CO₂/CH₄ molar ratios while it is hampered by high operating pressures [13]. Although the DRM process reduces CH₄ and CO₂ emissions into the atmosphere and converts them into a valuable product (syngas), it requires a quite high energy input because of two reasons. First, the elevated content of CO in the produced syngas results in an elevated total heating value compared to SMR syngas with a higher H₂ content [17]. Second, although DRM on paper is a simpler process than SMR as no steam is needed, the energy requirement is higher due to the exceptional thermodynamic stability of CO₂ [13–15,17–20].

CH₄ reforming processes are conventionally carried out in catalytic conditions [21]. Noble metals and group VIII metals (Ni, Fe, and Co) are active in both SMR and DRM [21–24]. However, Fe and Co are susceptible to oxidation under the harsh condition required for reasonably high conversions (high temperature and high steam pressure) while the application of noble metals is limited due to their high market price [6]. Consequently, Ni-based catalysts are extensively studied because of their cost-effectiveness and high reforming activity [25,26]. The main pitfall of using Ni-based catalysts is the very high coke formation rate, which generally causes a rapid failure of the catalysts [27–29]. The carbon deposits on the catalyst surface can have different forms (e.g., whisker, gum, pyrolytic coke) and they can seriously affect the reusability of the catalyst by disrupting the catalyst structure (Table 1) [30]. Gum-like (multilayer graphite) and pyrolytic coke can cover the active Ni sites and block the reaction whereas whisker carbon, having high mechanical strength, can break the catalyst pellet, hence causing a pressure build-up and tube failure [22]. Carbon can be formed via two main routes: methane decomposition (Equation (5)) and CO disproportionation (Equation (6)), the latter being dominant at low temperatures due to its exothermicity. When the reforming process is carried out at a high temperature, methane dissociation is the main source of coke buildup. The feed composition also influences the tendency to carbon accumulation. In general, low molar H/C and O/C ratios in the feed stream can promote coke generation [31]. The calculated H/C and O/C molar ratios of stoichiometric SMR are six and one, respectively, whereas in DRM feed they are lower (two and one, respectively), thus coke deposition is particularly more severe in DRM.

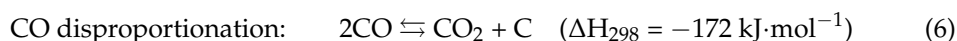
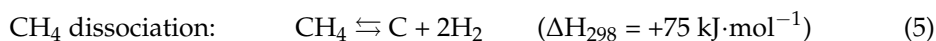


Table 1. Types of carbon formed during reforming reactions, their effects and critical conditions favoring the formation.

| Carbon Type | Effect on Catalysts | Effect on Reactor | Favored Conditions | Preventive Measures |
|----------------|--------------------------------------|--|--|---|
| Whisker carbon | Catalyst pellet break-up | Increase on pressure build-up | Feed of olefins and aromatics, low H ₂ O/C ratio, high operating temperature | Increase H ₂ O/C ratio |
| Gum | Deactivation by blocking active site | | Feed of aromatics, low H ₂ O/C ratio, absence of H ₂ , low operating temperature | Increase H ₂ O/C ratio Increase operating temperature H ₂ co-feed |
| Pyrolytic coke | Deactivation by blocking active site | Coke accumulation in reactor wall, increase on pressure build up | Feed of olefins, long residence time, high operating temperature, feed containing sulfur | Reduce residence time Remove sulfur from feed |

1.2. The Ni(M)/Mg(Al)O Catalysts

To overcome the identified challenges in catalytic reforming systems, the selection of the catalyst support plays a crucial role during the catalyst development [32–34]. In addition to coke limiting ability, reforming catalysts must also meet stringent requirements due to the harsh conditions required of the processes (high temperature, high pressure, and presence of steam) [22,35]. Common oxide supports are Al₂O₃, MgO, and their corresponding mixed oxides [22]. Because of its high surface area, thermal and chemical stability, and strong interaction with Ni, Al₂O₃ is one of the most studied supports [36,37]. Indeed, commercially available catalysts for traditional SMR are mainly constituted by Ni supported on Al₂O₃ [38]. MgO support is also widely studied, particularly in DRM, because its high basicity is beneficial for adsorbing CO₂, which in turn enhances the reforming activity and the coke removal rate [39,40]. Moreover, the ability of MgO to form a strongly interacting solid solution with NiO improves the catalyst stability and resistance to sintering [41,42]. Since these are all highly desirable characteristics for a support, the combination of Al and Mg oxides, that is, Mg-Al mixed oxides (herein denoted as Mg(Al)O), is often exploited to prepare highly performing catalysts and therefore will be discussed in the following sections [22,43].

As for the active metallic constituents, bimetallic systems are attracting considerable research interest thanks to the possible promotional effect of the second (or third) metal on the processes and/or the presence of synergetic effects between the metals [26,44,45]. Particularly for Ni-based catalysts, noble, alkaline, and rare earth metal promoters are the subjects of many studies and demonstrate promising improvements. Among those, the addition of small amounts of noble metals to Ni catalysts is beneficial while remaining cost competitive [31]. The addition of Pt, Ru, and Pd improves reducibility, may provoke an auto-activation of the catalyst, and reduces the coke formation [31]. On the other hand, the addition of Group 11 metals (Au, Ag) reduces the Ni activity but extends the catalyst's lifetime by inhibiting the coke formation [46].

In addition to the selection of the active metal, support, and promoters, the way the catalyst is prepared also plays an important role in determining its morphological and structural features and, as a result, its catalytic performance [46–48]. This is particularly true when preparing Mg-Al mixed oxides, which can form several crystal phases and can have different morphological characteristics [49,50]. Hence, a thorough understanding of each parameter in traditional synthesis procedures as well as the exploration of innovative preparation approaches are both highly desirable to improve homo- and bimetallic Ni catalysts supported on Mg(Al)O for SMR and DRM.

Metal–support interaction is arguably one of the most critical aspects impacting both the activity and the stability of heterogeneous catalysts, especially when used in high-temperature processes. The interaction of Ni with the support is a somewhat textbook example of the tradeoffs to be considered when preparing a heterogeneous catalyst. If,

on the one hand, a weak interaction is good for the catalytic activity because it does not impair the Ni reducibility, it may be insufficient to stabilize the nanoparticles against sintering [51,52]. It is also true, however, that it is hard to obtain small Ni nanoparticles, and thus a high number of catalytically active sites with Ni interacting too weakly with the support can be found. In other words, a strong interaction with the support helps suppress the overgrowth of the particles, thereby enhancing their stability at high reaction temperatures, but could also lead to Ni nanoparticles that are hard to reduce, which may limit the availability of metallic Ni [48,53].

The following section delves into the factors influencing the interaction of Ni with Mg and Al oxides separately and then with the Mg(Al)O mixed oxide.

2. Ni-Support Interaction in Ni(M)/Mg(Al)O Catalysts

Ni-based catalysts are generally prepared as NiO followed by reduction, but the final form of the catalyst is heavily influenced by the composition of the Mg(Al)O support because Ni interacts very differently with Al and Mg oxides. The metal–support interaction will be first discussed for Ni catalysts supported on Al and Mg oxides separately; then we will showcase a few examples of how their combination is essential to obtain high-performing reforming Ni-based catalysts.

NiO is known to form a stable spinel nickel aluminate with Al_2O_3 after heat treatment, denoted as NiAl_2O_4 [54]. In Ni–Al–O systems, three phases of Ni– Al_2O_3 can be observed: “free” NiO particles, NiO weakly interacting with Al_2O_3 , and NiAl_2O_4 spinel. The order is based on the strength of interaction between Ni and Al. Temperature-programmed reduction (TPR) can be used to identify the phases of Ni in Al_2O_3 (Figure 2). Due to the difference in bond strength, each phase displays reduction features in a specific temperature range. Reduction peaks occurring between 300 and 350 °C are originated by the reduction of “free” NiO to metallic Ni, whilst weakly interacting NiO– Al_2O_3 is reduced around 500–600 °C. The reduction of Ni^{2+} present in the spinel phase (NiAl_2O_4) can only be observed at temperatures higher than 800 °C. The formation of such three phases depends largely on calcination temperature, Ni loading, and the preparation method. Generally, high calcination temperatures favor the formation of spinel phases with stronger interaction between Ni and Al_2O_3 [55,56]. For instance, in catalysts containing 20 wt.% of Ni and calcined at temperature <750 °C, a low amount of the spinel phase could be detected, whereas Ni was present almost quantitatively as spinel when the catalyst was calcined at $T > 750$ °C. Salhi et al. found that the distribution of the spinel phase is also sensitive to the Ni/Al molar ratio [57]. In Ni-deficient samples, the solid exists as a mixture of Al_2O_3 and NiAl_2O_4 , whereas NiO aggregates are formed in materials with higher Ni content. The distribution of NiAl_2O_4 is also affected by the preparation method. For example, while comparing the phase composition between impregnated and co-precipitated catalysts, Li and Chen found that the co-precipitated sample showed less reducibility than the impregnated one, implying the formation of spinel NiAl_2O_4 by the former method [54].

With MgO, NiO can form an ideal NiO–MgO solid solution in the whole range of concentrations due to the similar ionic radii of Ni^{2+} (69 pm) and Mg^{2+} (72 pm) [58]. In the solid solution, the interaction of Ni with MgO is particularly strong, resulting in a Ni phase much harder to be reduced. Conventionally, the reduction of NiO–MgO occurs above 800 °C with long reduction times (Figure 3) [59]. Interestingly, the strong interaction between NiO and MgO facilitates the formation of small Ni nanoparticles (NPs) upon reduction, thus preventing particles sintering and coke formation [60,61]. Additionally, the high basicity of MgO could be beneficial for the stability of the catalyst by enhancing the absorption of oxidizing reagents (CO_2 , H_2O), resulting in better gasification of coke species formed on the catalyst surface [62,63].

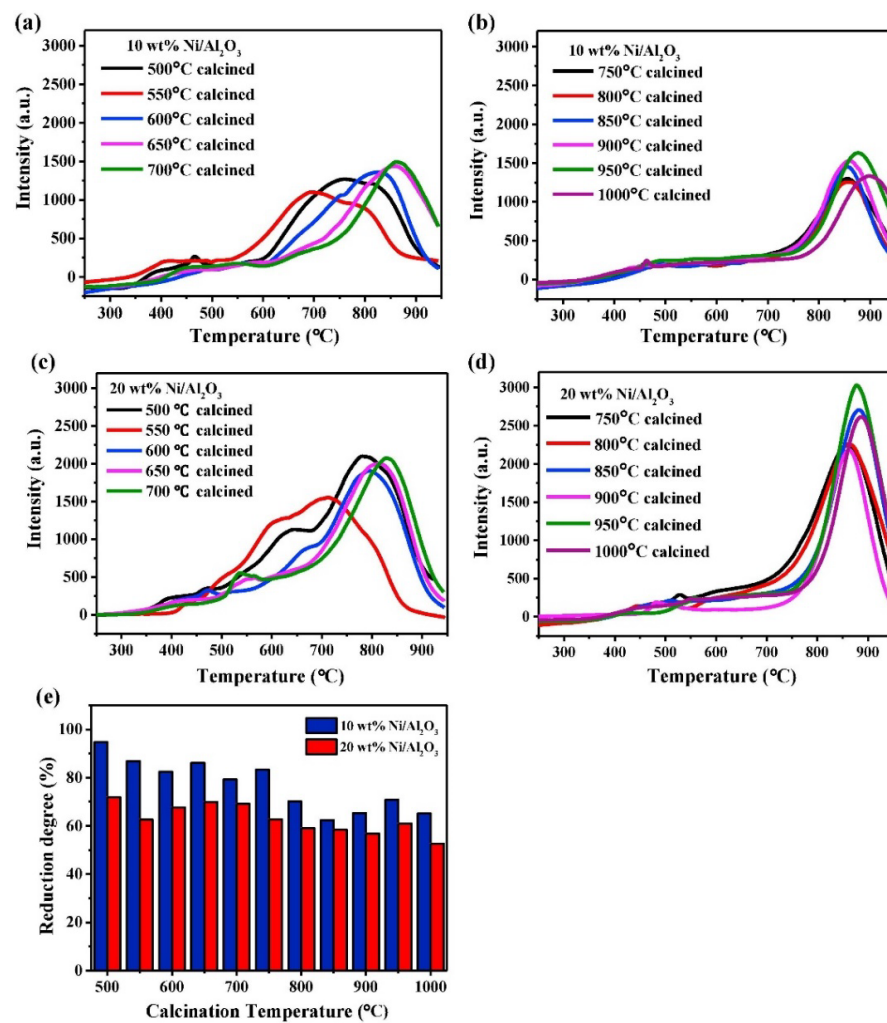


Figure 2. (a–e) TPR and reduction degree of Ni/Al₂O₃ with different loading and different calcination temperature. Reprinted with permission from [56], copyright 2018, Elsevier.

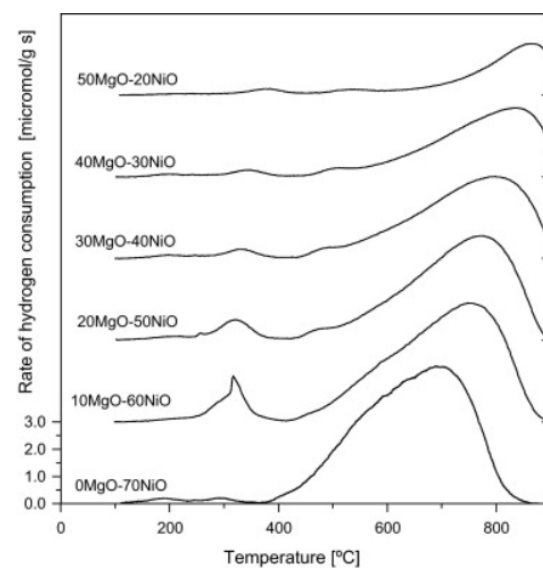


Figure 3. TPR of Ni-MgO samples with different loading of MgO. Reprinted with permission from [64], copyright 2011, Elsevier.

In addition to the interactions between Ni and each oxide component, the mixed oxide itself can also form the MgAl_2O_4 spinel phase during the catalyst synthesis [64,65], which provides high surface area, good thermal stability, and strong interaction with Ni [48]. Damyanova et al. prepared Ni catalysts for DRM with different ceramic-based supports (δ , θ - Al_2O_3 , SiO_2 - Al_2O_3 , ZrO_2 - Al_2O_3 , MgO - Al_2O_3) and the results indicated Ni/ MgO - Al_2O_3 as the most active and stable catalyst [66]. Zhang et al. tested various supports in DRM and they found that Al_2O_3 showed high stability while MgO exhibited great coke resistance [67]. Hence, the authors combined the two benefits by using MgO - Al_2O_3 mixed oxide as a support for Ni catalysts. The resulting material demonstrated good activity and was stable for over 100 h on stream. Mehr et al. showed that MgO addition reduces carbon deposition, likely due to the Lewis basicity of MgO [68]. It should be noted that Das et al. argued that basicity is not monotonically beneficial, but instead, an optimal acidic/basic balance is required for DRM catalysts [69]. The authors reported that basic sites favor the adsorption of CO_2 , while acidic sites are necessary for CH_4 activation.

Another important aspect of $\text{Mg}(\text{Al})\text{O}$ systems is the ability to form hydrotalcite. Hydrotalcite is a double-layered lamellar hydroxide (LDH) of Mg and Al with the formula $\text{Mg}_6\text{Al}_2(\text{OH})_{16}\text{CO}_3 \cdot 4\text{H}_2\text{O}$ [70]. It is demonstrated that materials derived from hydrotalcites are promising for various catalytic processes including CH_4 reforming [71,72]. By decomposing the precursors via thermal treatments, homogenized mixed oxides can be obtained. For Ni supported on $\text{Mg}(\text{Al})\text{O}$ catalysts, hydrotalcite-derived routes are a great way to obtain high surface area, tailored basicity, and uniform distribution of the active metal on the surface [73–78].

The first procedure to report is that described by Shishido et al., who named their method “solid phase crystallization” (spc) [77]. The procedure consisted of the replacement of Mg^{2+} with Ni^{2+} during the co-precipitation of the LDH precursor, followed by heat treatment to obtain the final catalyst. The authors found that with the spc approach, the catalysts had higher surface area and better dispersion than conventional impregnated samples. They also demonstrated that such catalysts performed well in SMR. Takehira et al. obtained similar results with the same spc approach and the $\text{Ni}_{0.5}/\text{Mg}_{2.5}\text{-Al}$ had high activity and stability under severe conditions of SMR. Moreover, they observed improved performance with the impregnated Ni/ Mg_3Al due to the reconstruction of the support towards the LDH-like structure during the impregnation process [79]. Further details on hydrotalcite-derived catalysts for SMR and DRM can be found in dedicated review papers [72,73,77,80].

3. Monometallic Ni/Mg(Al)O Catalysts for SMR and DRM

As discussed above, between the components of Ni-Mg-Al systems, various interactions can be established that can drive the efficiency and stability of the catalysts during the reaction. The preparation method therefore becomes crucial in obtaining the desired features. This section will discuss the conventional methods, that is, impregnation and co-precipitation, as well as more advanced techniques such as sol-gel, aerogel, atomic layer deposition (ALD), etc., highlighting the most critical synthesis parameters and their impact on catalytic performance [81].

3.1. Synthesis of Ni/Mg(Al)O Catalysts by Conventional Approaches

Ni catalysts supported on Al-Mg oxides obtained by impregnation and co-precipitation methods with different synthetic parameters, as well as their physicochemical properties and reforming performances for SMR and DMR processes, are summarized in Table 2 and discussed below. Particular attention is devoted to the role of the constituents and the thermal treatments of the catalysts (i.e., calcination and reduction steps).

Table 2. Monometallic Ni catalysts supported on Mg(Al)O obtained by co-precipitation and impregnation methods for SMR and DRM.

| Catalyst (Ni Loading wt.%) | Synthesis Method | Catalytic Process | Parameter Investigated ⁽¹⁾ | Reaction Conditions | Main Findings ⁽³⁾ | Ref. |
|--|--|-------------------|---------------------------------------|--|---|------|
| Ni/Al ₂ O ₃ (46.6–73.5 wt.%) | Co-precipitation | DRM | Ni/Al ratio | GHSV = 12 L g ⁻¹ h ⁻¹ CO ₂ /CH ₄ = 1 T = 400–700 °C ⁽²⁾ Max CH ₄ conv. = 90% (700 °C) | High Ni/Al ratio resulted in high reducibility and large particles Molar ratio Ni/Al = 2 showed the best result Higher calcination temperature resulted in higher activity | [82] |
| Ni/MgO (2–20 wt.%) | Impregnation on MgO nanosheets | DRM | Ni loading; (2–20 wt.%) | GHSV = 36 L g ⁻¹ h ⁻¹ CO ₂ /CH ₄ = 1 T = 450–650 °C Max CH ₄ conv. = 63% (650 °C) | High Ni loading resulted in larger particles Activity and stability increased with Ni loading from 2 to 10 wt.% Activity and stability decreased with Ni loading from 10 to 20 wt.% | [83] |
| Ni/3 wt.%MgO-Al ₂ O ₃ (5–20 wt.%) | Ni, Mg impregnation on sol-gel Al ₂ O ₃ | DRM | Ni loading (5–20 wt.%) | GHSV = 12 L g ⁻¹ h ⁻¹ CO ₂ /CH ₄ = 1 T = 550–700 °C Max CH ₄ conv. = 76% (700 °C) | High Ni loading led to segregation of NiO phase Coke formation was higher for higher Ni loadings | [84] |
| Ni/Mg(Al)O (2.5–15 wt.%) | Co-precipitation | DRM | Ni loading (2.5–15 wt.%) | GHSV = 18 L g ⁻¹ h ⁻¹ CO ₂ /CH ₄ = 1 T = 550–700 °C Max CH ₄ conv. = 74% (700 °C) | High Ni loading promoted NiO phase formation, improving reducibility Activity and coke formation proportionated to Ni content | [85] |
| Ni/Mg(Al)O (1–15 wt.%) | Impregnation on co-precipitated MgAl ₂ O ₄ | DRM | Ni loading (1–15 wt.%) | GHSV = 90 L g ⁻¹ h ⁻¹ CO ₂ /CH ₄ = 1 T = 750 °C Max CH ₄ conv. = 93% | High Ni loading improved reducibility, activity, and coke generation. Too low Ni loading (i.e., 1 wt.%) showed deactivation overtime | [43] |
| Ni/Mg(Al)O (4–60 wt.%) | Co-precipitation (LDH) | DRM | Ni loading (4–60 wt.%) | GHSV = 20,000 h ⁻¹ CO ₂ /CH ₄ = 1 T = 550–750 °C Max CH ₄ conv. = 90% (750 °C) | High Ni loading increased particles size, reducibility, and basicity No obvious sintering is presented after reaction High Ni loading promotes carbon formation. | [86] |
| Ni/Mg(Al)O (3–18 wt.%) | Co-precipitation | DRM | Ni loading (3–18 wt.%) | GHSV = 60 L g ⁻¹ h ⁻¹ CO ₂ /CH ₄ = 1 T = 500–800 °C Max CH ₄ conv. = 95% (800 °C) | Active site dispersion is optimal at Ni loading of 15 wt.% High CH ₄ conversion and CO disproportionation using high Ni loadings At high T _{reaction} , high Ni loading catalyst was more stable At low T _{reaction} , high Ni loading catalyst was less stable | [87] |
| Ni/Mg(Al)O (15 wt.%) | Co-precipitation (LDH) | SMR | Molar Ni/Mg-Al (2, 3, 4) | GHSV = 900 L g ⁻¹ h ⁻¹ H ₂ O/CH ₄ = 4 T = 650 °C Max CH ₄ conv. = 42% | Highest surface area, Ni dispersion was obtained with molar Ni/Mg-Al = 3 Molar Ni/Mg-Al = 3 showed highest activity in SMR | [88] |
| Ni/Mg(Al)O (6.3–12.6 wt.%) | Co-precipitation (spc) or impregnation | SMR | Synthesis method, molar Ni/Mg ratio | GHSV = 120 L g ⁻¹ h ⁻¹ H ₂ O/CH ₄ = 2 T = 800 °C Max CH ₄ conv. = 95% | Highest dispersion, best activity, and stability were observed with co-precipitated catalyst with a Ni/Mg molar ratio = 0.5/2.5 | [77] |
| Ni/Mg(Al)O (16.3 wt.%) | Co-precipitation (spc) | SMR | Molar ratio Mg/Al | GHSV = 180–900 L g ⁻¹ h ⁻¹ H ₂ O/CH ₄ = 2 T = 800 °C Max CH ₄ conv. = 98% | Low molar Mg/Al ratio resulted in Al(OH) ₃ and amorphous solid NiO-MgO and stable MgAl ₂ O ₄ Co-precipitated catalyst particles size remained after reaction Co-precipitated Ni _{0.5} /Mg _{2.5} -Al showed high activity, stable for 600 h | [79] |

Table 2. Cont.

| Catalyst (Ni Loading wt.%) | Synthesis Method | Catalytic Process | Parameter Investigated ⁽¹⁾ | Reaction Conditions | Main Findings ⁽³⁾ | Ref. |
|---|---|-------------------|---|--|---|------|
| Ni/Al ₂ O ₃ (5 wt.%) | Impregnation in mesoporous Al ₂ O ₃ | DRM | T _{cal} (500–800 °C) | GHSV = 120 L g ⁻¹ h ⁻¹ CO ₂ /CH ₄ = 1 T = 650–700 °C Max CH ₄ conv. = 78% (700 °C) | Calcination at 700 °C promoted spinel and limited NiO-Al ₂ O ₃ phase formation Too high calcination temperature (800 °C) reduced catalyst activity | [89] |
| Ni/Al ₂ O ₃ (3 wt.%) | Impregnation | DRM | T _{cal} (500–900 °C) T _{red} (500–800 °C) | GHSV = 2.6 L g ⁻¹ h ⁻¹ CO ₂ /CH ₄ = 1 T = 500–800 °C Max CH ₄ conv. = 85% (800 °C) | High T _{cal} reduced surface area but promoted basicity No difference in activity was observed with T _{cal} Reduction at lower than 700 °C showed no or little activity | [90] |
| Ni/Al ₂ O ₃ (10 wt.%) | Impregnation | DRM | T _{cal} , T _{red} | GHSV = 20 L g ⁻¹ h ⁻¹ CO ₂ /CH ₄ = 1 T = 500, 700 °C Max CH ₄ conv. = 87% (700 °C) | High T _{cal} promoted formation of spinel phase Calcination pretreatment did not affect activity and coke deposition Reduced catalyst minimized the coke deposition | [91] |
| Ni/Al ₂ O ₃ (16 wt.%) | Impregnation | DRM | T _{cal} (350–900 °C) | GHSV = 480 L g ⁻¹ h ⁻¹ CO ₂ /CH ₄ = 1 T = 500–800 °C Max CH ₄ conv. = NR | Catalyst calcined at 900 °C forms NiAl ₂ O ₄ . The catalyst was stable for 100 h TOS Strong Ni-Al interaction prevented particles being pushed by coke formed, reducing catalyst breakage. | [92] |
| Ni/Mg (20 wt.%) | Impregnation | DRM | T _{cal} (600–800 °C) | GHSV = 20 L g ⁻¹ h ⁻¹ CO ₂ /CH ₄ = 1 T = 800 °C Max CH ₄ conv. = 93% | High T _{cal} reduced interaction of Ni-MgO and reducibility No weakly interacting NiO when T _{calc} = 800 °C More CO ₂ adsorption site with increased T _{calc} Catalyst calcined at higher temperature is more active | [93] |
| Ni/MgO (13.1 wt.%) | Impregnation | DRM | Mg precursor T _{cal} of support | GHSV = 60 L g ⁻¹ h ⁻¹ CO ₂ /CH ₄ = 1 T = 790 °C Max CH ₄ conv. = 75% | [MgCO ₃] ₄ Mg(OH) ₂ precursor formed stable MgO at high T _{cal} Ni impregnated on [MgCO ₃] ₄ Mg(OH) ₂ showed highest CO yield Induction time to reach stable conversion depended on precursor and T _{cal} of support | [94] |
| Ni/Mg(Al)O (55 wt.%) | Co-precipitation | DRM | T _{cal} , T _{red} | GHSV = 1000 L g ⁻¹ h ⁻¹ CO ₂ /CH ₄ = 1.25 T = 800–900 °C Max CH ₄ conv. = 74% (900 °C) | Low T _{calc} resulted in rock-salt type with amorphous phase High T _{calc} resulted in spinel type with high crystallinity Reduction at 800 °C and 900 °C resulted in small nanoparticle (9 nm) Reduction at 1000 °C promoted sintering to large particles (19 nm) High reaction temperature resulted in lower coke formation | [95] |
| Ni/Mg(Al)O (15 wt.%) | Impregnation on LDH (MG30) | SMR | T _{cal} (350–1000 °C) | GHSV = 65 L g ⁻¹ h ⁻¹ P = 1–10 bar T = 600 °C H ₂ O/CH ₄ = 5 Max CH ₄ conv. = 50% | High T _{cal} reduced crystallite size Catalysts with T _{cal} lower than 650 °C deactivated with increased reaction pressure Optimal catalyst calcined at 850 °C | [96] |
| Ni/MoCeZr/MgAl ₂ O ₄ -MgO (10 wt.%) | Co-precipitation | DRM | T _{cal} | GHSV = 60 L g ⁻¹ h ⁻¹ CO ₂ /CH ₄ = 1 T = 900 °C Max CH ₄ conv. = 95% | Higher T _{cal} (900 °C) promoted MgAl ₂ O ₄ phase but decreased the surface area. NiAl ₂ O ₄ phase was not observed. At T _{cal} = 800 °C the catalyst showed the highest activity and stability | [97] |

Table 2. Cont.

| Catalyst (Ni Loading wt.%) | Synthesis Method | Catalytic Process | Parameter Investigated ⁽¹⁾ | Reaction Conditions | Main Findings ⁽³⁾ | Ref. |
|-----------------------------|----------------------------------|-------------------|--|---|---|------|
| Ni/Mg(Al)O (22.3–50.3 wt.%) | Co-precipitation | DRM | Molar Mg/Al, Ni/Mg ratio T _{cal} (550–700 °C) T _{red} (550–700 °C) | GHSV = 45 L g ⁻¹ h ⁻¹ CO ₂ /CH ₄ = 2 T = 500–700 °C Max CH ₄ conv. = 92% (700 °C) | Surface area was independent from Ni content but decreased with low molar Mg/Al ratio Reduction, but not calcination, affected the activity Mg/Al affected activity more than Ni/Mg Reduction temperature enhances activity and H ₂ selectivity Low Mg/Al molar ratio negatively affected the activity | [98] |
| Ni/Mg(Al)O (2.5–10 wt.%) | Co-precipitation or Impregnation | DRM | T _{cal} , T _{red} , preparation method | GHSV = 15 L g ⁻¹ h ⁻¹ CO ₂ /CH ₄ = 1 T = 700–800 °C Max CH ₄ conv. = 97% (700 °C) | High T _{cal} reduced specific surface area and dampened reducibility Activity decreased when catalyst was treated at high T _{cal} Ni-Mg/Al by co-precipitation showed good resistance to coke Ni/MgO by impregnation showed higher activity than co-precipitation | [99] |

⁽¹⁾ T_{red}: Reduction temperature, T_{cal}: Calcination temperature; ⁽²⁾ When not mentioned, reaction pressure is atmospheric; ⁽³⁾ Highest conversion reported among investigated catalysts; NR: not reported.

3.1.1. Effect of Ni Loading and Composition Ratio

Ni loading and composition ratio play an important role in the characteristics of the catalysts: High Ni loadings may imply higher activity, but they may result in larger particles, which promote coke formation [82,83,100–102].

The study by Guo et al. showed that a catalyst with a low Ni content is not stable in DRM, while the conversion is positively correlated with Ni content only up to 15 wt.% [43]. As expected, above that loading, the coke formation becomes severe. A similar trend of coke deposition was found by Alipour et al. while studying impregnated Ni/Mg(Al)O catalysts obtained by wet impregnation [84]. They showed that after calcination, NiO segregated when above the 15 wt.% of Ni loading. The amount of carbon deposited scaled with the Ni content, but the reforming activity did not. Catalysts prepared via co-precipitation showed a similar behavior [85]. Akbari et al. synthesized mesoporous nanocrystalline Ni-Mg-Al catalysts using that method and studied the effect of Ni loading in DRM. They found again that Ni loading up to 15 wt.% did not dramatically change the textural properties of the catalysts (pore volume, pore size distribution, and surface area) and that above that loading the catalysts experienced severe coke deposition.

Some other studies focused on investigating which pathway of coke formation is preferred with the change in Ni content. Dėbek et al. tested co-precipitated Ni/Mg(Al)O catalysts with up to 60 wt.% Ni loading in DRM and they found that the higher the Ni content, the higher the CH₄ conversion [86]. Surprisingly, no improvement in CO₂ conversion was observed when the Ni content changed. The authors indicated that the marginal increment of CH₄ conversion is due to CH₄ decomposition, resulting in an increase in coke deposited. Characterization of the Ni-rich catalysts showed large and highly reducible particles, along with a low basicity, which could cause coke formation. The Ni content is also found to affect the CO disproportionation pathway contribution [87]. Lin et al. investigated similar Ni/Mg(Al)O catalysts and found a positive correlation between reforming conversion as well as CO disproportionation activity and Ni loadings at a lower range (3–18 wt.%). In their study, at a low reaction temperature (600 °C), Ni-rich samples significantly promoted the coke deposition via the CO pathway, hindering the stability of the catalysts. At high reaction temperature (750 °C), where the exothermic Boudouard reaction is suppressed, the reverse relationship was observed: Catalysts containing more active metal showed better stability and less coke deposition.

Qi et al. used Ni/Mg(Al)O prepared by the co-precipitation technique and tested them in SMR in comparison with wet impregnated catalysts with varied divalent/trivalent cation molar ratios (Ni+Mg)/Al in the precursors [88]. They reported that the optimal (Ni+Mg)/Al molar ratio in the LDH precursor for SMR is three. The resulting catalyst exhibited the best activity because of its high surface area and high Ni dispersion upon reduction. A similar optimal (Ni+Mg)/Al molar ratio was found by Takehira et al. in SMR by co-precipitated Ni-Mg-Al [79]. The authors found that the high Al content can result in segregated Al(OH)₃ and amorphous NiO-MgO, which are detrimental to the catalyst activity and stability. The optimal molar ratio between Ni and Mg (Ni/Mg = 0.5/2.5) was tested and was stable for 600 h. Shishido et al. also found that Ni/Mg = 0.5/2.5 molar ratio gave the highest dispersion for the co-precipitated Ni-Mg-Al catalyst [77].

3.1.2. Effect of Heat Treatment

Both calcination and reduction conditions have a major impact on the physicochemical properties of the resulting catalyst. As stated earlier, higher calcination temperatures favor the formation of stable phases, such as spinel NiAl₂O₄ or NiO-MgO solid solution. A high calcination temperature can enhance the stability and interaction between components but can also decrease the surface area, thus causing a collapse of the pores, and particle sintering [103–106]. On the contrary, low reduction temperatures may not guarantee the generation of sufficient active species (Table 3). Hence, various studies have been devoted to the influence of thermal pretreatments on the final structure of the catalysts.

Table 3. General effects of synthesis conditions on Ni/Mg(Al)O catalysts.

| Synthesis Conditions | Advantages | Disadvantages |
|------------------------------|--|---|
| High calcination temperature | <ul style="list-style-type: none"> - More stable catalyst by favoring the formation of the spinel phase | <ul style="list-style-type: none"> - Decrease in the surface area - Less exposed Ni - Promotes sintering - Decreases reducibility |
| High reduction temperature | <ul style="list-style-type: none"> - Activates catalyst - More metallic Ni | <ul style="list-style-type: none"> - Creates large particles - Promotes sintering |
| High Ni loading | <ul style="list-style-type: none"> - More active catalyst - Increases reducibility - Increases basicity | <ul style="list-style-type: none"> - Creates larger particles - Promotes sintering - Promotes coke formation |

Bian et al. studied the effect of the calcination temperature on the activity of Ni catalysts supported on Al₂O₃ [89]. They found that high calcination temperatures promote the interaction between Ni and Al and the formation of the spinel phase. The activity and stability of Ni/Al₂O₃ were optimal when calcined at 700 °C. Higher calcination temperatures added no improvements to the catalysts' activity. However, in another study, Al-Fatesh et al. argued that the reduction is the step most crucial to activate the catalysts in DRM [90]. The best catalyst that the authors reported was calcined at 900 °C and reduced at 700 °C. Juan-Juan et al. found also that pretreatment influences the coke formation on Ni/Al₂O₃ in DRM [91]. The uncalcined but reduced catalyst gave the least amount of carbon during the reaction, due to its smaller Ni NPs compared to the calcined and reduced one. Coke deposition dependence on thermal treatment was also studied by Zhou et al. [92]. They observed that the calcination temperature affects the phase distribution of Ni/Al₂O₃ as higher temperature favors spinel formation. They proposed that spinel phases limit the formation of encapsulated carbon, thus resulting in a stable activity.

The calcination temperature was studied on NiO-MgO systems for DRM [93,107]. At low calcination temperatures, the material contained weakly interacting NiO species, while at 800 °C NiO bonds strongly with MgO in the form of a solid solution. The strong interaction increases the strength of CO₂ absorption at low reaction temperatures, thus enhancing the activity and stability of the catalyst. The effect of Mg precursors and heat treatment was also studied by Ruckenstein and Hu [94]. It was observed that the morphology of MgO before Ni impregnation is important to determine the activity and induction time in DRM. Among the investigated systems, the catalyst prepared from [MgCO₃]₄ Mg(OH)₂ precursor through a high calcination temperature protocol carried out in a short time was the optimal catalyst due to high Ni dispersion on the surface of the support.

Katheria et al. investigated the effect of the calcination temperature on Ni/MgAl₂O₄ in SMR [96]. The authors argued that when a higher calcination temperature is used, smaller Ni crystallites form upon reduction. They attributed such behavior to the strong metal-support interaction generated by the high calcination temperature. The catalyst was most active when calcined at 850 °C, whereas at 1000 °C the activity decreased because of a partial loss of Ni surface due to the incorporation of Ni into an inactive bulk spinel phase. Surprisingly, a different conclusion was drawn by Li et al. [98]. In their study on a complex Ni/Mo-Ce-Zr/MgO-Al₂O₃ catalyst for DRM, they proposed that the low activity of the catalyst calcined at elevated temperature is to be ascribed to particle sintering. They suggested that high calcination temperatures (900 °C) promote the migration of Ni from stable NiO-MgO solid solution to spinel MgAl₂O₄. This mobility enables Ni enrichment on the surface upon reduction, thus stimulating particle enlargement. The authors emphasized that an optimal calcination temperature prevents the formation of large particles.

For co-precipitated catalysts, the reduction condition turns out to be more influential than the calcination condition [95,98]. Perez-Lopez et al. found that with co-precipitated Ni-Mg-Al catalysts, the calcination temperature had a limited effect on the activity, mostly by altering the specific surface area of the material [98]. A similar relationship was observed by Djaidja et al. [99]. In addition, the authors reported that a high reduction temperature (up to 700 °C) was beneficial for the catalysts' activity as it increased the number of active sites. However, sintering can occur at very high reduction temperatures [95]. Mette et al. found that a reduction temperature up to 900 °C did not affect the particle size of Ni but sintering of Ni NPs was observed when the reduction temperature reached 1000 °C.

In summary, different studies show that the effects of Ni loading and pretreatment conditions are complex and possess both advantages and disadvantages. Table 3 sums up the general trends based on the works discussed above. Careful consideration must be given to the calcination and reduction steps. In general, thermal treatments at high temperatures are preferred since they promote the formation of stable phases while an elevated reduction temperature provides activation of the catalysts. Nevertheless, excessive heat treatments can be detrimental causing surface area reduction, sintering of particles, and formation of inactive species. It should be noted that high-temperature treatments need high energy inputs, which could limit the economic viability of the final catalyst.

3.2. Synthesis of Ni/Mg(Al)O Catalysts by Advanced Methods

Besides the more common methods mentioned above, other approaches aimed at obtaining strictly controlled morphological, structural, and textural properties of both the metal active phase and the support have been explored and are here summarized (Table 4).

Among them, the sol-gel method has been extensively investigated [108–111]. The catalysts obtained via this approach are typically characterized by high surface area, narrow size distribution, high thermal resistance, and homogeneous composition of the mixed oxides when compared to conventional synthesis methods [112,113]. González et al. utilized LDHs prepared in this way as precursors for DRM [114]. Upon mild thermal treatment, the hydrotalcite collapsed and formed nanosphere structures of mixed NiO and Mg(Ni)AlO periclase without the formation of NiAl₂O₄. The catalyst with 15 wt.% Ni and calcined at 650 °C showed the best activity and low carbon formation in DRM. Sahli et al. used a sol-gel-like method with propionic acid to synthesize Ni-Al oxides for DRM [115]. By varying the ratios between Ni and Al, sub-stoichiometric Ni/Al resulted in a high-surface area solid solution of Al₂O₃ and NiAl₂O₄, which was stable for the reaction. Stoichiometric Ni/Al and Ni-excess samples resulted in a segregated NiO phase, which was completely deactivated due to coke formation. Min et al. compared Ni/Mg(Al)O prepared by sol-gel synthesis to the co-precipitated counterpart in DRM. The authors found that the sol-gel catalysts formed a lower amount of coke [116]. They also studied the effect of various Mg/Al molar ratios on catalyst performance. The coke resistance ability of the catalysts was improved by increasing the MgO loading, whereas high activity was expressed at Mg/(Mg+Al) molar ratio from 0.44 to 0.86. The authors attributed the excellent performance to the high surface area of the catalyst and the high dispersion of Ni.

The Pechini method, which is based on the incorporation of metal precursors into a polymeric resin, allows for the preparation of highly controlled and uniform multicomponent phases [117,118]. Rogers et al. used the Pechini method to synthesize Ni-Al catalysts with different molar Ni/Al ratios for both DRM and SMR [119]. By this method, they obtained highly uniform, structurally crystalline, and small grain-sized aluminate. They found that the Ni-rich catalyst (denoted as Ni₂Al₂O₅) featured both NiO and NiAl₂O₄ phases. In SMR, the active phase was likely reduced Ni NPs but, surprisingly, unreduced stoichiometric NiAl₂O₄ was also active for DRM without the presence of metallic Ni. By X-ray absorption spectroscopy (XAS) analyses, the authors concluded that four-fold-coordinated Ni²⁺ is responsible for the activity and low carbon deposition of the examined catalyst.

Another attractive synthesis approach is the aerogel method. This approach enables the synthesis of exceptionally high surface area and thermally stable materials [120].

Suh et al. used aerogel Al_2O_3 as supports for DRM [121]. The high surface area Al_2O_3 was prepared by supercritical CO_2 drying of alcogels. The aerogel-based Ni/ Al_2O_3 catalysts showed high activity and enhanced stability against coking compared to the impregnated ones. The authors assigned such improvements to the high surface area and uniform distribution of the active sites. The follow-up paper investigated the metal loading on this aerogel catalyst, again highlighting that too a high metal content resulted in large particle sizes, which in turn promote coke formation [101].

Sebai et al. sought to improve the traditional incipient wetness by complexing a Ni precursor with aliphatic amine before impregnation [122]. The authors hypothesized that the high steric hindrance of aliphatic amine limits the growth of NiAl_2O_4 , resulting in smaller Ni particle sizes. Indeed, they reported that the average Ni particle size decreased (13 nm to 9 nm) when a bulkier ligand (trialkylamine) was used. High reactivity in SMR was recorded for catalysts using N-triethylamine as a complexing agent.

Atomic layer deposition (ALD) allows for high control of the catalyst surface and might open new pathways for synthesizing stable catalysts [123]. Zhang et al. used this method to prepare Ni/porous $\gamma\text{-Al}_2\text{O}_3$ for DRM [124]. The catalyst showed higher activity at 850 °C than the one made by wet impregnation but took 10 h to reach its stable conversion. The authors claimed that the ALD synthesis results in spinel NiAl_2O_4 , whose time-consuming reduction was behind the long induction period of the catalyst. Interestingly, they reported that the pretreatment with pure H_2 at 700 °C gave no DRM activity, whereas the product stream (H_2 and CO) at 850 °C could reduce the spinel phase leading to catalytic activity. Wang et al. reported ALD-made catalysts with remarkably superior activity and stability compared to the impregnated counterparts but came up with a different explanation [125]. They attributed the poor performance of the impregnated samples to the presence of a NiAl_2O_4 spinel phase, whereas ALD samples contained more NiO, which is easier to reduce, thus resulting in higher activity. The ALD approach was also used for the preparation of NiO-MgO and specifically to improve the basicity of the catalysts [126]. Jeong et al. also utilized the ALD approach to overcoat Ni NPs with MgO. With 200 ALD cycles, the basicity of the catalyst was greatly enhanced. In CO_2 -TPD, the control sample contains weak and moderate basic surface sites ($0.7 \mu\text{mol CO}_2/\text{g}_{\text{cat}}$ desorbed around 170–400 °C) while 200-ALD-cycled catalysts comprise mostly strong basic sites ($1.04 \mu\text{mol CO}_2/\text{g}_{\text{cat}}$ desorbed around 450–700 °C). The activity and stability of this catalyst were higher than the bare NiO and overcoated 50-ALD-cycled MgO/NiO. Other studies demonstrated that ALD-prepared catalysts present a significant improvement in sintering resistance and stability. Gould et al. synthesized Ni/ Al_2O_3 with an overlayer of porous Al_2O_3 by molecular layer deposition (MLD) to stabilize the catalyst during DRM [127]. The resulting catalysts were less affected by sintering thanks to the presence of the overcoat. The activity and stability of the catalysts depended significantly on the calcination and reduction temperature. The catalyst with 10 MLD cycles showed high stability with repeated calcination and reduction cycles, and no deactivation over a long running time (up to 108 h) was observed. In another work on ALD-synthesized Ni/ Al_2O_3 catalysts, Littlewood et al. reported that the overcoated catalysts were more resistant to sintering and coke formation compared to uncoated samples [128]. The authors found that the pretreatment of overcoated samples affects the induction time to reach maximal activity since the overlayers restructure themselves through the transformation of inactive spinel NiAl_2O_4 to active metallic Ni under the reaction stream.

The importance of thermal treatments was stressed also by Kim et al. while preparing Ni catalysts via one-pot evaporation-induced self-assembly (EISA) [129]. They found that the right annealing conditions are vital to obtaining improved morphological and structural characteristics (such as smaller and more dispersed Ni NPs) and, in turn, a superior catalytic activity in SMR.

Table 4. Monometallic Ni catalysts supported on Mg(Al)O obtained by advanced methods for SMR and DRM.

| Catalyst (Ni Loading) | Synthesis Method | Catalytic Process | Reaction Conditions ⁽¹⁾ | Main Findings | Ref. |
|--|---------------------------------|-------------------|--|---|-------|
| Ni/Mg(Al)O (4.3–19.0 wt.%) | Sol-gel | DRM | GHSV = 120 L g ⁻¹ h ⁻¹ CO ₂ /CH ₄ = 1 T = 800 °C ⁽²⁾ Max CH ₄ conv. = 98% | Sol-gel hydrotalcite formed periclase instead of spinel phase upon calcination Catalysts from sol-gel precursor calcined at 650 °C possessed the best activity and low carbon formation. | [114] |
| Ni/Al ₂ O ₃ (30.4–52 wt.%) | Sol-gel | DRM | GHSV = 30 L g ⁻¹ h ⁻¹ CO ₂ /CH ₄ = 1 T = 700–800 °C Max CH ₄ conv. = NR | Sol-gel method enabled homogeneous and stoichiometric spinel formation. Ni-rich catalysts contained separated Ni particles, promoting carbon formation | [115] |
| Ni/Mg(Al)O (15 wt.%) | Sol-gel | DRM | GHSV = 72 L g ⁻¹ h ⁻¹ CO ₂ /CH ₄ = 1 T = 800 °C Max CH ₄ conv. = 90% | Sol-gel Ni/Al ₂ O ₃ showed poor activity and high coke formation Sol-gel Ni/MgO showed high activity despite low reducibility Sol-gel Ni/Mg(Al)O obtained the highest activity and steady performance | [116] |
| Ni/Al ₂ O ₃ (20–45 wt.%) | Pechini method | DRM | GHSV = 52,400 h ⁻¹ CO ₂ /CH ₄ = 1 T = 700 °C Max CH ₄ conv. = 43% | Highly uniform, highly crystalline, and grain-sized NiAl ₂ O ₄ were formed Unreduced stoichiometric spinel NiAl ₂ O ₄ was active for DRM | [119] |
| Ni/Al ₂ O ₃ (20–45 wt.%) | Pechini method | SMR | GHSV = 65,500 h ⁻¹ H ₂ O/CH ₄ = 2.4 T = 700 °C Max CH ₄ conv. = 82% | Highly uniform, highly crystalline, and grain-sized NiAl ₂ O ₄ were formed Reduced Ni particles were active for SMR | [119] |
| Ni/Al ₂ O ₃ (10 wt.%) | Aerogel | DRM | GHSV = 24 L g ⁻¹ h ⁻¹ CO ₂ /CH ₄ = 1 T = 700 °C Max CO ₂ conv. = 60% | High surface area support and uniformed active sites were prepared by supercritical CO ₂ drying Higher loading of Ni in aerosol catalysts led to higher coke formation | [121] |
| Ni/Al ₂ O ₃ (6 wt.%) | Impregnation of Ni-complex | SMR | GHSV = 24 L g ⁻¹ h ⁻¹ H ₂ O/CH ₄ = 3 T = 500–800 °C Max CH ₄ conv. = 99 % (800 °C) | Complexing Ni before impregnation hindered particle growth Ni-triethylamine performed well in SMR | [122] |
| Ni/Al ₂ O ₃ (1 wt.%) | Atomic layered deposition (ALD) | DRM | GHSV = 34 L g ⁻¹ h ⁻¹ CO ₂ /CH ₄ = 1 T = 700–850 °C Max CH ₄ conv. = 99% (850 °C) | ALD catalysts showed higher activity than impregnated ones. ALD catalysts required a longer induction period | [124] |
| Ni/Al ₂ O ₃ (0.8–2 wt.%) | ALD | DRM | GHSV = 7.2 L g ⁻¹ h ⁻¹ CO ₂ /CH ₄ = 1 T = 400–800 °C Max CH ₄ conv. = 80% (800 °C) | ALD catalysts contained more NiO, resulting in higher activity compared to impregnated catalysts | [125] |
| Ni/MgO (NR) | ALD | DRM | GHSV = 12 L g ⁻¹ h ⁻¹ CO ₂ /CH ₄ = 1 T = 800 °C Max CH ₄ conv. = 73% | MgO-deposited catalysts obtained higher basicity The activity and stability of the catalysts were greatly enhanced with ALD | [126] |

Table 4. Cont.

| Catalyst (Ni Loading) | Synthesis Method | Catalytic Process | Reaction Conditions ⁽¹⁾ | Main Findings | Ref. |
|--|------------------------------|-------------------|---|---|-------|
| Ni/Al ₂ O ₃ (0.8 wt.%) | Molecular layered deposition | DRM | GHSV = 30 L g ⁻¹ h ⁻¹ CO ₂ /CH ₄ = 1 T = 700 °C Max CH ₄ conv. = 38% | MLD catalysts exhibited sintering resistance 10 MLD cycled catalyst was stable up to 108 h time of stream | [127] |
| Ni/Al ₂ O ₃ (2 wt.%) | ALD | DRM | GHSV = 72 L g ⁻¹ h ⁻¹ CO ₂ /CH ₄ = 1 T = 700 °C Max CH ₄ conv. = 39% | ALD catalysts show higher stability compared to spinel NiAl ₂ O ₄ Induction time was required for ALD to restructure the overlayer to active Ni species | [128] |
| Ni/Mg(Al)O (not found) | EISA | SMR | GHSV = 10 L g ⁻¹ h ⁻¹ H ₂ O/CH ₄ = 3 T = 800 °C Max CH ₄ conv. = 97.6% | The most active catalyst prepared via sequential inert-air thermal treatments | [129] |
| Ni/Mg(Al)O | CAHD | DRM | GHSV = 96 L g ⁻¹ h ⁻¹ CO ₂ /CH ₄ = 1 T = 700 °C Max CH ₄ conv. = 79% | CAHD catalysts had higher surface area, uniform pore size, high basicity, and small Ni nanoparticle (2.1 nm) The activity and stability of the catalysts were higher than the co-impregnated Ni/MgO-Al ₂ O ₃ catalyst. | [130] |
| Ni/Mg(Al)O (LDH) | Freeze drying | DRM | GHSV = 480 L g ⁻¹ h ⁻¹ CO ₂ /CH ₄ = 1 T = 800 °C Max CH ₄ conv. = 93% | Freeze drying preserved LDH-like platelet structure and resulted in higher Ni dispersion. Freeze dried catalysts showed higher activity (rate 8.3 mmol CH ₄ s ⁻¹ g-cat ⁻¹ at 900 °C) and higher coke resistance | [131] |
| Ni/Mg(Al)O (12 wt.%) | Impregnation + 3D printing | SMR | GHSV = 6 L g ⁻¹ h ⁻¹ H ₂ O/CH ₄ = - T = 800 °C Max CH ₄ conv. = 75% | Ni impregnated on a 3D printed support with a binder for large-sized reactors | [132] |
| Ni/Mg(Al)O (8 wt.%) | Co-precipitation | SMR | GHSV = 2.5 L g ⁻¹ h ⁻¹ H ₂ O/CH ₄ = 1.8 T = 700 °C Max CH ₄ conv. = 93.2% | Coke deposition after 350 h on stream of 0.32 wt.% Catalyst molded into 2.5 mm diameter spherical beads | [133] |

⁽¹⁾ When not mentioned, reaction pressure is atmospheric; ⁽²⁾ Highest conversion reported among investigated catalysts; NR: not reported.

Recently, Guo et al. synthesized Ni supported on Mg-Al-O by so-called cation-anion double hydrolysis (CADH) for DRM [130]. The preparation is done based on the simultaneous hydrolysis of Ni^{2+} and Mg^{2+} cations with AlO_2^- cation in an aqueous solution. The resulting catalyst possesses high surface area, uniform pore size, high basicity, and ultrasmall Ni nanoparticles upon reduction (2.1 nm). When compared with co-impregnated Ni/MgO-Al₂O₃ (Ni and Mg were co-impregnated on γ -Al₂O₃) in DRM, the CADH catalyst showed both higher initial activity and long-term stability. TOF of the CADH catalyst was calculated as 23.9 s⁻¹, twice as much as conventional Ni/MgO-Al₂O₃. Moreover, virtually no coke was observed during 24 h TOS while the co-impregnated catalyst showed high coke formation accompanied by steady deactivation. The authors attributed the high activity and exceptional coke resistant property to small-sized Ni nanoparticles and enhanced CO₂ activation thanks to the high basicity created by the preparation method.

The utilization of the freeze-drying method was investigated by Huang et al. [131]. In their study, Ni was co-precipitated with Mg and Al precursors to form an LDH structure, followed by freeze drying instead of conventional oven drying. The authors claimed that freeze drying helps preserve the platelet-like structure of parent LDH, thus improving the surface area and pore size distribution. The resulting catalysts, containing small Ni nanoparticles with high dispersion, performed exceptionally in DRM with high WHSV, up to 8.3 mmol CH₄ s⁻¹ g-cat⁻¹. In the stability test, the freeze-dried catalysts showed higher coke resistance compared to oven-dried samples. The strong interaction between precursor species, accompanied by preserved highly porous morphology and uniform distribution of Ni species, was claimed to be a crucial factor for observed improvement.

In general, these less conventional synthesis methods have proved very useful in amplifying specific attributes of the final catalysts, such as the surface area (sol-gel, aerogel), phase distribution (sol-gel, Pechini method, ALD), Ni dispersion (sol-gel, Pechini method, precursor complexation), basicity (ALD), and sintering resistance (ALD), allowing researchers to understand how they impact on the reforming process. For example, in DRM, it turned out that high stability should be sought by enhancing the Ni-MgO interaction and/or by using the Al-containing phase to increase the surface area.

Scaling up the preparation of a catalyst, also taking into consideration the final shape of the material in a way that can be used in industrial applications, is often a difficult endeavor. Worth mentioning are two patents where two different approaches are disclosed with interesting results. In the first, spherical beads of the catalysts of 2.5 mm in size showed steady activity for about 350 h on stream thanks to particularly stable Ni NPs of 10 nm in size [132]. In the second, it is disclosed that 3D-molding approaches using different kinds of binder are a good way to produce active catalysts in shapes suitable for large reactors [133].

4. Bimetallic Ni-M/Mg(Al)O Catalysts for Reforming Reactions

4.1. Bimetallic Ni-M/Mg(Al)O Catalysts for SMR

Bimetallic catalysts are a promising area of research because they have improved properties compared to their parent metals, resulting in some cases in catalysts with higher selectivity, activity, and stability. Precious metals with high reforming activity and low coking tendency have been studied as promoters for Ni-based catalysts [134–139]. Among different synthesis methods reported for CH₄ reforming catalysts (i.e., self-combustion, ion exchange, sol-gel, microemulsion, precipitation, wet impregnation, and colloidal), precipitation and impregnation methods are the most common ones [140–144].

The role of Pt as a promoter in Ni/Mg(Al)O catalysts has been investigated in different synthetic ways both for metal deposition and support preparation. Foletto et al. reported a catalyst synthesized by the sequential impregnation method while using the sol-gel method via alkoxide hydrolysis to synthesize the Mg(Al)O support [145]. XRD analyses revealed that as the calcination temperature of the support increased, the size of the crystallites rose exponentially, and the formation of the spinel phase occurred at temperatures higher than 600 °C. The formation of the pure spinel phase and a higher resistance to sintering were observed for calcination temperatures exceeding 700 °C. The catalytic activity of the

catalyst as a function of different Pt content showed that 0.1 wt.% Pt is optimal compared to catalysts at higher Pt loadings. According to TPR results, Ni reduction peaks shifted to lower temperatures for small amounts of Pt (0.05–0.1 wt.%), while no significant changes were observed when increasing the Pt content.

The activity and stability of catalysts obtained by sequential Ni and Pt impregnation were studied by Jaiswar et al. [146]. MG30 (Sasol, 30 wt.% MgO: 70 wt.% Al₂O₃) was used as support, which experienced a weight loss of about 40 wt.% after the heat treatment due to the conversion of aluminum magnesium hydroxyl carbonate to Mg(Al)O [96]. The effect of Pt doping on Ni/Mg(Al)O catalysts was investigated with different Pt concentrations (0.01, 0.05, 0.1, 0.3, and 1.0 wt.% Pt) and 15 wt.% of Ni. According to the TPR results performed on the calcined samples, the reduction peak appeared at about 800 °C, which was higher than the reduction peak observed for Ni/Al₂O₃ catalysts doped with Pt and prepared with co-impregnation [147,148]. One reason for this could be the presence of MgO on the catalyst support, which might lead to a strong interaction between the metal oxide and the support itself [149,150]. The different Pt loadings showed that the crystallite size of the active metal increased up to 0.1 wt.%, accompanied by some agglomeration of the active metals on the support. The H₂ uptake study also revealed a positive correlation between metal dispersion and Pt loading up to 0.1 wt.%, which was confirmed by TEM analysis. From the TEM images of 0Pt15Ni, 0.1Pt15Ni and 1.0Pt15Ni catalysts (the names referring to 0, 0.1, and 1.0 wt.% Pt, respectively), smaller NPs were observed for the 0.1Pt15Ni catalyst, while larger agglomerated ones were present in the 0Pt15Ni catalyst (Figure 4). In agreement with the dispersion of the active metals after the addition of Pt, the activity was the highest with the 0.1 wt.% Pt-doped Ni/Mg(Al)O catalyst. Higher Pt concentrations led to agglomeration of the active metal, resulting in lower catalytic activity.

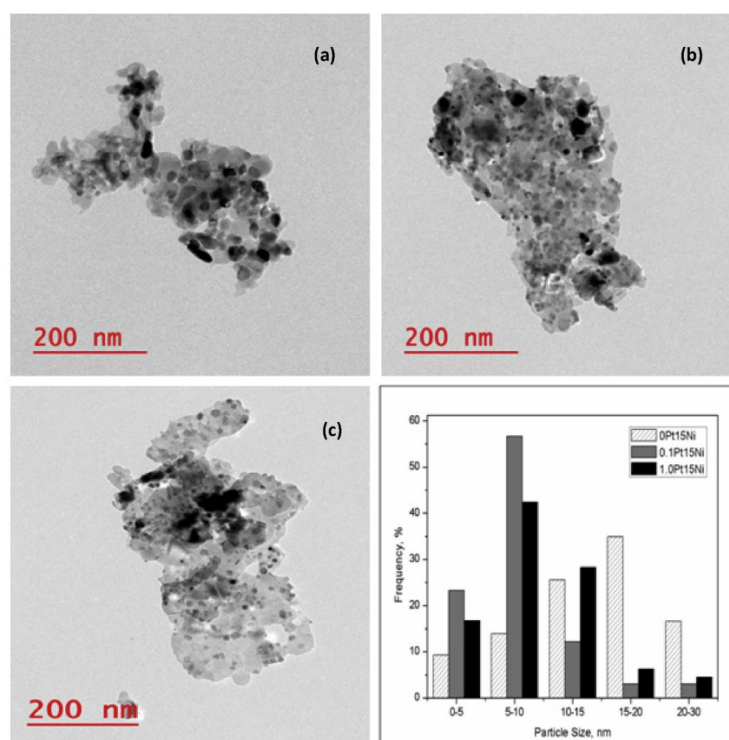


Figure 4. TEM images and active metal particle size distribution for (a) 0Pt15Ni, (b) 0.1Pt15Ni, and (c) 1.0Pt15Ni catalysts. Reprinted with permission from [146]. Copyright 2017, Elsevier.

Katheria et al. investigated Rh-Ni/Mg(Al)O catalysts prepared by sequential impregnation, designated as cat600600, cat600850, cat850600, cat850850 (the names referring to the first and second calcination temperatures) and co-impregnation referred to as RhNicoimp calcined at 600 °C [151]. The catalysts prepared by both methods showed the highest activ-

ity at lower calcination temperatures (calcined at 600 °C in each step). Basically, above that temperature, and regardless of the presence of Rh, hard-to-reduce Ni aluminate (NiAl_2O_4) formed, as can be seen in the UV-Vis spectra in Figure 5, which limited the catalytic activity. An improvement in the activity and stability of the catalysts was nonetheless observed after Rh loading mainly due to an increment of the reduction degree, dispersion of the active metals, and the formation of Rh-Ni alloy. It is noteworthy that Rh exerted a similar promoting behavior to Pt. Specifically, Rh loadings up to 0.1 wt.% led to an enhancement in the initial CH_4 conversion and H_2 yield, while further amounts had no significant effect.

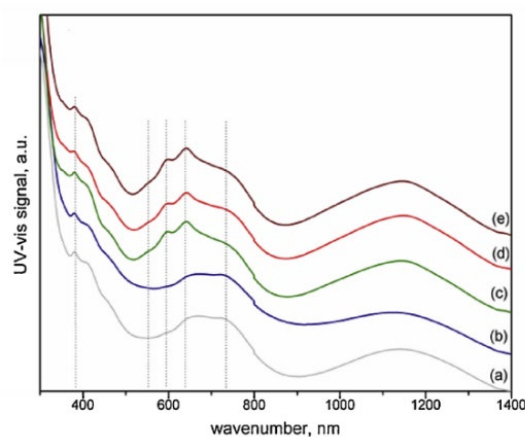


Figure 5. UV-vis spectroscopic patterns of (a) RhNicoimp, (b) Cat600600, (c) Cat600850, (d) Cat850600, and (e) Cat850850. Reprinted with permission from [151], copyright 2019, Elsevier.

With due care [152], another factor to be considered in catalysts doped with Rh and Pt is the hydrogen spillover effect [153–155]. Kinetic studies indeed showed that noble metals can promote the adsorption of the H_2 formed during the reaction, which then spill over the non-noble metal thus contrasting its oxidation [155,156]. The presence of Pt-group metals in bimetallic formulations has the positive effect of facilitating the reduction of Ni as well as preventing its undesired oxidation during reforming operations.

Ru-doped Ni catalysts, effective for SMR without the prereluction treatment, were reported by Jeong et al. [157]. They investigated the effect of the addition of Ru to $\text{Ni}/\text{Al}_2\text{O}_3$ and $\text{Ni}/\text{Mg}(\text{Al})\text{O}$ prepared by sequential impregnation under the same conditions. For both catalysts, Ru suppressed the carbon deposition and had a self-activation effect on the oxidized catalysts during reforming; Ni catalysts without Ru, on the contrary, were active only after reduction of the catalysts. As in the case of monometallic Ni catalysts (see Section 2), this study proved also that Ru-Ni/Mg(Al)O is more active than Ru-Ni/ Al_2O_3 , likely due to the presence in the latter of Ni species that are hard to reduce because they are dispersed as alluminates. In another study on a similar system, the self-reducibility was ascribed to the H_2 spillover that occurred after the addition onto reduced NiO species under the reaction conditions, so that a very small amount of Ru (0.05 wt.%) exerted a positive effect on the conversion of CH_4 [158]. The best-performing catalyst showed remarkable stability without deactivation in a long test over a period of 250 h.

Nawfal et al. studied in a more systematic way the effect of Ru on $\text{Ni}_x\text{Mg}_{6-x}\text{Al}_2$, with $x = 2, 4,$ and 6 molar ratios [159]. Mixed oxides based on Ni, Mg, and Al were synthesized by the hydrotalcite route and then Ru was added via an impregnation method. Among the different catalysts tested, Ru/ Ni_6Al_2 showed the best performance, attributed essentially to the stronger interaction between Ru and Ni as the former promotes the reducibility of the NiO species (Figure 6).

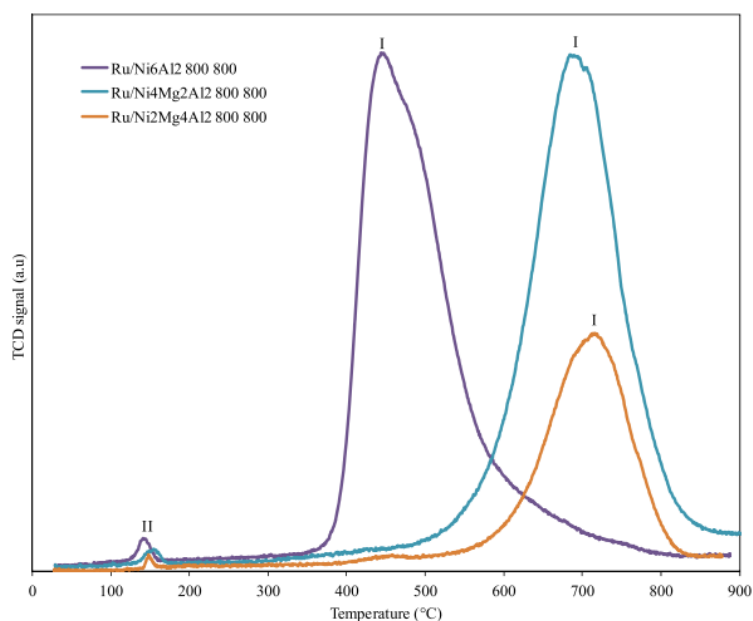


Figure 6. TPR profiles of Ru/Ni_xMg_{6-x}Al₂ samples (x = 2, 4 and 6). Reprinted with permission from [159], copyright 2015, Elsevier.

Kim et al. investigated the use of non-noble promoters for SMR with physically mixed Ni/Mg(Al)O + CrFe₃O₄ catalysts [160]. They noted that when Cr or Fe was added to the Ni/Mg(Al)O catalyst via classical sequential impregnation, Ni segregated, thus compromising the catalytic activity. On the contrary, the authors reported increased activity with the physically mixed catalysts that could be due to a more facile water activation by CrFe₃O₄. The recent case of a NiCo catalyst prepared via the one-pot evaporation-induced self-assembly method (EISA) whose activity is markedly higher than the parent monometallic counterpart [161] is notable. Although these catalysts were evaluated at relatively low space velocities (see Table 5 for a comparison with other catalysts), this work shows that co-precipitation methods or similar are a promising way to control the formation and alloying of Ni-M nanoparticles, thus unlocking some perks typical of bimetallic formulations such as a higher presence of catalytically active metal(s) [45,162]. Attempts at preparing active Ni-M catalysts through other procedures have resulted only in a very slightly better coke resistance [163].

Small amounts (<0.5 wt.%) of alkaline metals, such as Ca and Sr, have been reported as beneficial in suppressing the coke formation during the reaction of SMR but only in the presence of CO₂, that is, simulated natural gas [164,165].

Not all noble metals promote Ni activity though. Indeed, Au-Ni/Mg(Al)O catalysts for SMR prepared by sequential impregnation revealed that the addition of a small amount of Au on Ni-based catalysts caused a decrease in H₂ chemisorption and dissociative N₂O adsorption, which can be mainly attributed to the effect of Au on the adsorption properties of several adjacent Ni sites [166]. Calculations showed that Au is usually located at step and edge sites, which are active sites for catalytic activity but can also serve as sites for carbon nucleation [167,168]. This study showed that the addition of 0.4 wt.% Au to 8.8 wt.% Ni/Mg(Al)O resulted in a small decrease in catalyst activity (Figure 7).

Table 5. Bimetallic Ni catalysts supported on Mg(Al)O for SMR.

| Catalyst (M ₁ /M ₂) | Synthesis Method | Reaction Conditions ⁽¹⁾ | Main Finding | Ref |
|--|--|--|---|-------|
| Pt-Ni/Mg(Al)O (0.1 wt.%/15 wt.%) | Sequential impregnation; Support: obtained by sol-gel method, calcined at 1100 °C | GHSV = 9.6 L g ⁻¹ h ⁻¹ H ₂ O/CH ₄ = 4 T = 600 °C ⁽²⁾ Max CH ₄ Conv. = 80% | - The catalytic activity of Ni/Mg(Al)O was significantly improved by the addition of Pt. - There is a proportional relationship between CH ₄ conversion and metal surface area. | [145] |
| Pt-Ni/Mg(Al)O (0.1 wt.%/15 wt.%) | Sequential impregnation; Support: Commercial MG30, calcined at 900 °C | GHSV = 83 L g ⁻¹ h ⁻¹ H ₂ O/CH ₄ = 5 T = 600 °C Max CH ₄ Conv. = 65% | - 0.1 Pt wt.%-doped catalyst showed the maximum dispersion of active metals. - At higher concentrations of Pt on the metal surface, agglomeration of active metals occurred. - The addition of Pt increased the CO selectivity and decreased the H ₂ /CO ratio. | [146] |
| Rh-Ni/Mg(Al)O (0.5 wt.%/15 wt.%) | Sequential impregnation; Support: Commercial MG30, calcined at 900 °C | GHSV = 83 L g ⁻¹ h ⁻¹ H ₂ O/CH ₄ = 5 T = 600 °C Max CH ₄ Conv. = 59.2% | - The addition of 0.1 Rh wt.% to Ni/Mg(Al)O significantly increased the catalytic activity. - Further addition of Rh had no significant effect on the initial catalytic activity. - The sequentially impregnated catalyst showed better activity than the catalyst prepared via the co-impregnated method and calcined at 600 °C. | [151] |
| Ru-Ni/Mg(Al)O (0.5 wt.%/20 wt.%) | Sequential impregnation; Support: co-precipitated, calcined at 900 °C | GHSV = 160 L g ⁻¹ h ⁻¹ H ₂ O/CH ₄ = 1.2 T = 650 °C Max CH ₄ Conv. = NR | - Mg(Al)O-supported catalysts were more active than Al ₂ O ₃ -supported ones in the reforming reaction. - NiO species are more dispersed and reducible on Mg(Al)O compared to NiO species on Al ₂ O ₃ . | [156] |
| Ru-Ni/Mg(Al)O (0.1 wt.%/12 wt.%) | Stepwise impregnation; Co-impregnation; Support: commercial MG30 | GHSV = 50 L g ⁻¹ h ⁻¹ H ₂ O/CH ₄ = 3 T = 700 °C Max CH ₄ Conv. = 89% | - A trace amount of Ru (0.05 wt.%) addition over Ni/Mg(Al)O catalyst showed excellent self-activation property. - Impregnation of Ni in the first step showed better catalytic activity especially at lower temperatures compared to sequential impregnation of Ni after Ru. | [158] |
| Ru/Ni ₄ Mg ₂ Al ₂ (0.5 wt.%) Ru/Ni ₂ Mg ₄ Al ₂ (0.5 wt.%) | Co-precipitation followed by Impregnation; Support: Coprecipitation, calcined at 800 °C | GHSV = 6 L g ⁻¹ h ⁻¹ H ₂ O/CH ₄ = 1 T = 650 °C Max CH ₄ Conv. = 76% | - Ru not only facilitated the reducibility of NiO species but also increased their amount. - Ru-Ni interaction was higher in the catalyst with higher Ni content and so the activity increased. - The presence of Mg is not necessary and Ru-Ni interaction is sufficient to obtain high activity and selectivity. | [159] |

Table 5. Cont.

| Catalyst (M ₁ /M ₂) | Synthesis Method | Reaction Conditions ⁽¹⁾ | Main Finding | Ref |
|--|--|--|---|-------|
| Fe-Ni/Mg(Al)O (1 wt.%/15 wt.%) Cr-Ni/Mg(Al)O (1 wt.%/15 wt.%) Ni/Mg(Al)O + CrFe ₃ O ₄ (15 wt.%/10 wt.%) | Sequential dry impregnation; Support: Commercial MG70 | GHSV = 3000 h ⁻¹ H ₂ O/CH ₄ = 2 T = 700 °C Max CH ₄ Conv. = 84% | - Promoted catalysts showed smaller Ni particle sizes but increased the formation of segregated Ni metal and resulted in a negative effect on activity. - Physically mixed catalyst showed superior performance in CH ₄ conversion and H ₂ selectivity, but lower CO ₂ selectivity. | [160] |
| NiCo/MgAl ₂ O ₄ (15 wt.%/5 wt.%) | EISA | H ₂ O/CH ₄ = 1 T = 700 °C GHSV = 10 L g ⁻¹ h ⁻¹ Max CH ₄ Conv. = ~84% | - Ni-Co alloy formed upon reduction - Ni reduction favored by Co | [161] |
| Ni-Ca/Mg(Al)O (20 wt.%/0.35 wt.%) | Co-precipitation and impregnation | H ₂ O/CH ₄ /CO ₂ = 1.63/1/0.6 T = 900 °C GHSV = 3000 h ⁻¹ Max CH ₄ Conv. = 83.2% | - Steam methane reforming of carbon dioxide reaction - Ca suppresses the coke deposition | [164] |
| Ni-Sr/Mg(Al)O (16 wt.%/0.8 wt.%) | Impregnation | GHSV = 1200 h ⁻¹ H ₂ O/CH ₄ = 2.5 T = 750 °C Max CH ₄ conv. = 69.3% | - Steam reforming of simulated natural gas - Catalyst prepared by kneading method in the presence of calcium aluminate as cement | [165] |
| Au-Ni/Mg(Al)O (0.4 wt.%/8.8 wt.%) | Wet Impregnation; Support: Commercial MG30, calcined at 700 °C | GHSV = 3300 L g ⁻¹ h ⁻¹ H ₂ O/CH ₄ = 1 T = 550 °C Max CH ₄ Conv. = 6.4% | - Au had an electronic effect on the adsorption properties of several adjacent Ni sites. - The addition of Au to the catalyst resulted in a decrease in the formation of graphitic carbon during SMR. | [166] |
| Pt-Ni/Mg _{3.5} Al ₂ O ₄ (0.05 wt.%/10 wt.%) | sequential impregnation; Support: commercial Mg-Al with Mg/Al molar ratios of 3.5, 1.3 and 0.5 | GHSV = 1600 L g ⁻¹ h ⁻¹ H ₂ O/CH ₄ = 2 T = 600 °C Max CH ₄ Conv. = 42.6% | - Pt and Rh-doped Ni/[Mg _{3.5} Al]O catalysts showed stable activity during (daily start-up and shut-down) DSS operations. - The 0.05 wt.% Pt/10 wt.% Ni/[Mg _{3.5} Al]O catalysts were self-activated and exhibited self-regenerative activity in the DSS operations. | [169] |

⁽¹⁾ When not mentioned, reaction pressure is atmospheric; ⁽²⁾ Highest conversion reported among investigated catalysts; NR: not reported.

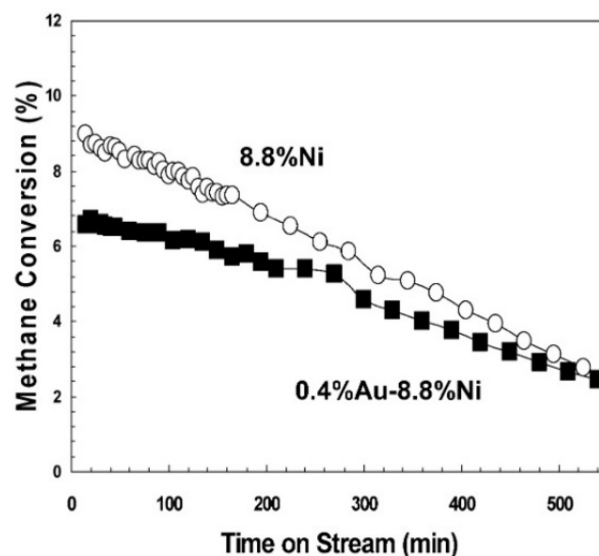


Figure 7. SMR activity over 8.8 wt.% Ni/Mg(Al)O (O) and 0.4 wt.% Au–8.8 wt.% Ni/Mg(Al)O (■). Reaction conditions: 550 °C, $\text{H}_2\text{O}/\text{CH}_4/\text{H}_2 = 4.5/4.5/1$, 3.3×10^6 cc/(h g). Reprinted with permission from [166], copyright 2006, Elsevier.

4.2. Bimetallic Ni-M/Mg(Al)O Catalysts for DRM

The presence of a metallic phase is necessary for the dissociative adsorption of CH_4 and for the generation of H_2 as well as chemisorbed carbon species during DRM. Some bimetallic systems are also capable of lowering the activation energy of the rate-limiting step [170,171]. A kinetic study by Niu et al. revealed that the addition of Pt to Ni reduces the activation energy for CH_4 dissociation and lowers moderately the CO_2 dissociation barrier energy, resulting in higher catalytic activity [172]. Re and Ru have been also described as active sites for CO_2 activation, which, due to their electron-rich properties, can donate electrons to the CO_2 antibonding orbitals and facilitate the reaction by weakening the C–O bond [173]. In addition, the dilution effect of the noble metal leads to higher metal dispersion, smaller particle size, and improves reducibility and oxidation resistance [174].

Ru, Pt, and Rh generally exhibit higher catalytic activity and stability compared to Ni due to their resistance to coke deposition [175–177]. Wu et al. investigated the effect of Pt and Au over Ni/ Al_2O_3 and Ni/ Al_2O_3 - MO_x ($\text{M} = \text{Ce}$ or Mg) oxides synthesized by the sequential wet impregnation method [178]. Bimetallic Ni–Pt, Ni–Au, and trimetallic Ni–Au–Pt catalysts were prepared over pure Al_2O_3 and Al_2O_3 loaded with 10 wt.% MgO and CeO. The addition of Au and Pt promoted the Ni reduction, while only 0.2 wt.% Pt and Au was sufficient to suppress the coke formation, which was more evident in the case of the trimetallic formulation. In detail, in the monometallic Ni/ Al_2O_3 catalyst, at least two types of carbon, namely amorphous carbon and carbon nanotubes, were found after the catalytic tests. The presence of MgO in the support was reported to suppress the formation of the amorphous type while in the case of CeO, carbonaceous species in the form of nanotubes were also observed. Bamboo-like carbon structures were found only in the most active catalyst, that is, Ni–Au–Pt/ Al_2O_3 . Moreover, particle size distributions for Ni/ Al_2O_3 and Ni–Au–Pt/ Al_2O_3 after a long run were measured and Ni–Au–Pt/ Al_2O_3 was characterized by a narrower particle size distribution and by the presence of smaller metallic NPs.

In another impregnation synthesis process, Pt was loaded on a Ni/Mg(Al)O catalyst using glow discharge plasma pretreatment after impregnation and before calcination [179]. Such treatment was useful to improve the Ni dispersion but inhibited its reduction. The addition of Pt helped in this sense and in fact the bimetallic, plasma-treated Pt–Ni/Mg(Al)O catalyst demonstrated a higher conversion of both the reactant and a higher H_2 yield. An improved resistance toward coke formation was also reported by the authors. The presence of Pt resulted in smaller Ni NPs in the fresh materials, while the plasma treatment was critical to prevent

sintering. It is worth noting the filamentous carbon formations on the spent Ni/Mg(Al)O catalyst, which on the contrary cannot be seen on the spent P-Ni-Pt/Mg(Al)O catalyst. The authors suggest that this was due to the presence of Pt more than the plasma treatment, and specifically to an altered dissociative adsorption capacity of CH₄ [180,181].

In a different way, the effect of Pt on Ni/Mg(Al)O catalysts was investigated by the combination of DFT and kinetic studies [172]. In that work, Pt was added to the supported Ni catalyst by a redox reaction. The remarkable feature of this synthesis method is that a very fine size of the Ni NPs can be obtained, likely because the reduced Ni is dissolved in the solution and then redispersed on the support during the redox reaction. For four catalyst models, the adsorption of key intermediates during the reaction was investigated by DFT calculations. The study showed that the energy barriers for both CH and C oxidation were lower after Pt loading, and the energy barrier for CH decomposition leading to surface carbon was higher after Pt loading, demonstrating the effect of Pt in the improvement of the catalytic performance and coke resistance.

The combination of Ni and Co as bimetallic catalysts and their synergistic effect on coke resistance was studied by Li et al. [182]. They attempted to develop a catalyst with high performance by controlling multiple factors including the size of the NPs, the interaction between the support and metal, the structure of the catalyst, and the alloying effect. The catalysts were prepared by co-precipitation in three different metal loadings. Increasing the Ni content of the catalyst resulted in an improved activity, in agreement with the study of Hu et al. [183]. They reported that at low Ni loadings, MgO surrounded the reduced metallic Ni atoms and limited the formation of Ni-Ni bonds and thus prevented the formation of Ni NPs. Metallic NPs of Ni and Co formed a bimetallic alloy, resulting in a more stable catalyst during DRM operations compared to the monometallic Ni catalyst. Since Co can hardly be reduced from its oxides or solid solutions, it can be employed to control the size of Ni NPs. Moreover, the elemental assignment of NiCo₂(4,6)/Mg_{0.9}(Al)O showed that the Ni and Co atoms were uniformly distributed into the metal NPs. The size of the metal NPs was close to that of the support in this catalyst, so this nanocomposite structure led to a stronger interaction between the metal NPs and the support. Recently, Duan et al. found that calcination and reduction of Ni-Co-Mg-Al hydrotalcite synthesized by the coprecipitation method yields fine Ni-Co alloy particles with uniform composition [184]. Ni-Co-Mg-Al hydrotalcite decomposes into a solid Mg(Ni,Co,Al)O solution during calcination, resulting in the incorporation of Ni and Co cations into the MgO lattice, and the subsequent reduction step produces an alloy with a similar Ni:Co ratio in the bulk composition. They showed that the prepared Ni-Co alloy effectively inhibited the decomposition of methane and improved the catalytic stability. Moreover, the increment of Co content in the Ni-Co alloy has a direct effect on the removal of the formed carbon species by enhancing the adsorption of CO₂ on the metal particle and/or at the metal-support interface.

In general, many alloying effects of Ni-based catalysts with base metals and Ni-based catalysts with noble metals have been reported in DRM and SMR to improve the dispersion and reducibility of the supported metal, modify the catalytic performance such as activity and selectivity, and improve the resistance to carbon deposition, sulfur poisoning, sintering, and so on (see Table 6). However, the effects of alloys often vary with catalysts, compositions, and reaction conditions [185].

Ru was combined with various metals such as Cr, Fe, Co, Ni, and Cu by Tsyganok et al. using a novel method based on the ability of Mg(Al)O oxide to reconstruct a layered structure following the memory effect of calcined hydrotalcite when rehydrated with aqueous solutions [186–188]. Traditionally, LDHs are prepared by co-precipitation of Mg²⁺ and Al³⁺ cations at basic pH. Since LDH can incorporate and retain inorganic and organic anions, Ni was used as the anionic species in a complex with ethylenediaminetetra acetic acid [M(EDTA)]^{n−}. After calcination, the first metal was introduced into the support as an anionic chelate by exploiting the memory effect of the calcined hydrotalcite, then the catalyst was calcined again, and the second metal (in this case Ru) was introduced into the catalyst pre-chelated EDTA (Figure 8). In this process, the chelated Ru³⁺ reduced to

atomic species and then sintered to form metallic clusters. When the metallic Ru clusters reached a suitable size, they began to catalyze the dissociation of CH_4 to C and H, which in turn can reduce the Ni oxide crystals by binding to the support surface near the Ru clusters. Catalysts obtained from this LDH showed high and sustained catalytic activity for the DRM reaction.

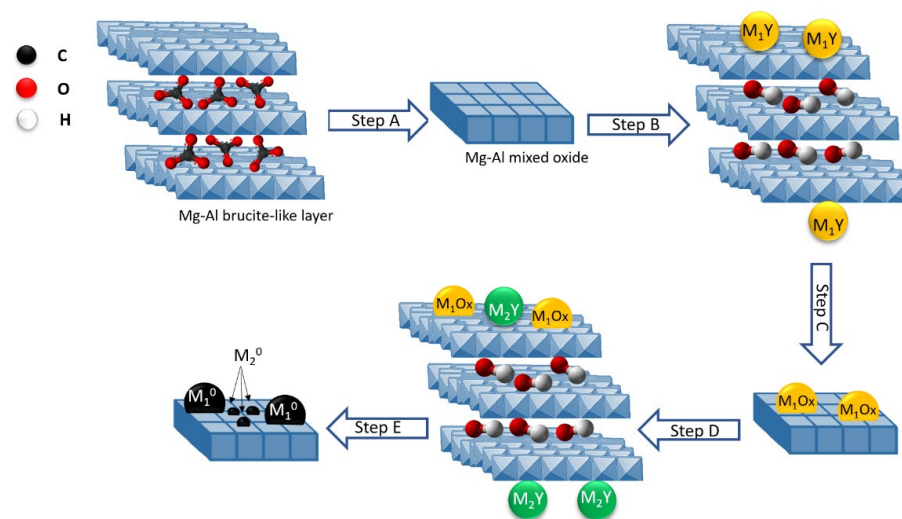


Figure 8. Synthetic strategy of preparing bimetallic catalysts, supported on Mg–Al mixed oxide: calcination of synthetic hydrotalcite in air at 500 °C to Mg(Al)O mixed oxide (step A), introduction of a transition metal M_1 as an anionic chelate (M_1Y^-) using a “memory effect” of calcined HT (step B), second calcination in air at 500 °C (step C), reconstruction of a layered structure and introduction of a second metal M_2 , i.e., Ru(III) pre-chelated with EDTA (step D), and an in situ generation of a bimetallic (M_2 – M_1) catalyst from LDH precursor under the DRM reaction conditions (step E). Reprinted with permission from [186], copyright 2005, Elsevier.

The influence of different supports on the catalytic activity of Ni and Ru–Ni catalysts was studied by Wysocka et al. [189]. They prepared bimetallic Ru–Ni catalysts by impregnation and precipitation methods. The highest activity was obtained with those supports that strongly interact with the active metals and have basic properties, which favor the dissociative adsorption of CO_2 on the catalyst [5,42]. Thus, the highest activity was observed for Ni/ Al_2O_3 and Ni/Mg(Al)O catalysts, where the addition of Ru particles improved the CH_4 conversion and shifted the H_2/CO molar ratio to lower values.

The influence of the support on Rh-modified Ni catalysts synthesized by wet impregnation was studied by Lucrédio et al. [190]. The presence of the noble metal, surprisingly, was detrimental to the catalytic activity mostly because of severe coke deposition. On the Al_2O_3 support the presence of Rh probably caused the segregation of Ni species with time-on-stream; on the Mg(Al)O support, the presence of Rh enhanced the dispersion of Ni by reducing the Ni^0 crystallite size, but the Rh–Ni/Mg(Al)O sample still suffered from higher rates of carbon deposition, suggesting that the carbon deposition in this case was due to CH_4 decomposition by Rh.

The evaluation of Fe–Ni catalysts synthesized via incipient wet impregnation found a sweet spot at a Fe/Ni molar ratio equal to 0.7 as the most active and least deactivated catalyst [191]. Crystallographic structural studies of bimetallic Fe–Ni/Mg(Al)O catalysts revealed that Fe_2O_3 and NiO were reduced to a Fe–Ni alloy in the presence of H_2 above 634 °C, and this alloy decomposed to metallic Ni and Fe_3O_4 during CO_2 oxidation above 627 °C. A Mars–van Krevelen mechanism was proposed for DRM based on in situ XRD and pulse experiments over Fe/Mg(Al)O, Ni/Mg(Al)O, and Fe–Ni/Mg(Al)O catalysts. Accordingly, CO_2 oxidizes Fe to FeO_x , and CH_4 is activated at Ni sites to form H_2 and surface carbon. Carbon can be re-oxidized from FeO_x by lattice O, leading to CO (Figure 9).

Table 6. Bimetallic Ni catalysts supported on Mg(Al)O for DRM.

| Catalyst (M ₁ /M ₂ wt.%) | Synthesis Method | Reaction Conditions ⁽¹⁾ | Main Finding | Ref. |
|---|---|---|---|-------|
| Pt-Ni/Mg(Al)O (0.5 wt.%/12 wt.%) Pt-Ni/Mg(Al)O (1 wt.%/12 wt.%) | Redox reaction (Pt ²⁺ + Ni → Pt + Ni ²⁺); Support: Ni/Mg/Al obtained by co-precipitation, calcined at 600 °C | GHSV = 360 L g ⁻¹ h ⁻¹ CO ₂ /CH ₄ = 1 T = 700 °C Max CH ₄ Conv. = 65% | - The Pt–Ni bimetallic catalysts enhanced activity, selectivity, and coke resistance. - The kinetic study showed that the bimetallic catalyst by reducing the activation energy of methane, resulting in higher activity. | [172] |
| Ni-Pt/Al ₂ O ₃ (4 wt.%/0.2 wt.%) Ni-Au/Al ₂ O ₃ (4 wt.%/0.2 wt.%) Ni-Au-Pt/Al ₂ O ₃ (4 wt.%/0.2 wt.%) Ni-Au-Pt/Mg(Al)O (4 wt.%/0.2 wt.%) | Sequential impregnation; Support: Sol-gel | GHSV = 60 L g ⁻¹ h ⁻¹ CO ₂ /CH ₄ = 1 T = 700 °C (²) Max CH ₄ Conv. = 86.8% | - The addition of Au and Pt leads to an increasing reduction of NiO species and catalytic activity. - The addition of MgO (10 wt.%) to Al ₂ O ₃ has no positive effect on the activity of the trimetallic catalyst. | [178] |
| Pt-Ni/Mg(Al)O (0.1 wt.%/8 wt.%) P-Pt-Ni/Mg(Al)O (0.1 wt.%/8 wt.%) | Impregnation and glow discharge plasma pretreatment; Support: co-precipitation | GHSV = 72 L g ⁻¹ h ⁻¹ CH ₄ /CO ₂ = 1 T = 550 °C Max CH ₄ Conv. = 31.7% | - Pt on Ni/Mg(Al)O catalyst promoted the reduction of Ni, but plasma pretreatment does not improve it. - The P-NiPt/Mg(Al)O catalyst showed high reforming activity due to the increase in Ni particle dispersion, and it exhibited strong resistance to coking and sintering. | [179] |
| NiCo ₂ /Mg _{0.9} (Al)O (1.7 wt.%/2.92 wt.%) NiCo ₂ /Mg _{0.9} (Al)O (2.79 wt.%/5.17 wt.%) | Co-precipitation; Support: co-precipitation | GHSV = 120 L g ⁻¹ h ⁻¹ CH ₄ /CO ₂ = 1:1 T = 700 °C Max CH ₄ Conv. = 55% | - The catalyst has a nanocomposite structure that resulted in high coke resistance and long-term on-stream stability for DRM. - The formation of Ni-Co alloy and the difficulty of Co reduction from solid solution affected the performance of the catalyst. | [182] |
| Ni ₃ Co ₉ /Mg(Al)O (2.38 wt.%/7.13 wt.%) | Co-precipitation Support: Co-precipitation, Calcination: 800 °C, for 15 h, Reduction: 800 °C | GHSV = 120 L g ⁻¹ h ⁻¹ CH ₄ /CO ₂ = 1:1 T = 750 °C Max CH ₄ Conv. = 88% | - The Ni-Co alloy effectively inhibits methane decomposition and coke deposition, resulting in a significant improvement in catalytic DMR stability. - Presence of Co enhances the metal-support interaction. | [184] |
| Ru-Ni/Mg(Al)O _x (0.1 wt.%/5.0 wt.%) | Reconstruction reaction using aqueous solutions of pre-chelated metals; Support: Co-precipitation, calcination: 500 °C, for 16 h | GHSV = 35 L g ⁻¹ h ⁻¹ CH ₄ /CO ₂ = 1:1 T = 800 °C Max CH ₄ Conv. = 94% | - Catalyst was generated in situ from LDHs under the DRM reaction conditions. - Catalyst showed high activity, no induction time upon in situ generation, and low coking ability. | [186] |

Table 6. Cont.

| Catalyst (M ₁ /M ₂ wt.%) | Synthesis Method | Reaction Conditions ⁽¹⁾ | Main Finding | Ref. |
|---|---|--|--|-------|
| Ru-Ni/Al ₂ O ₃ (0.6 wt.%/8 wt.%) Ru-Ni/Mg(Al)O (0.6 wt.%/7 wt.%) | Impregnation; Support: Co-precipitation, Calcined at 400 °C, for 6 h | GHSV = NR CH ₄ /CO ₂ = 1:1 T = 800 °C Max CH ₄ Conv. = 100% | - The highest activity was observed in support strongly interacting with Ni particles. - Introduction of Ru particles into the process system led to a shift in the ratio of H ₂ to CO to lower values because of enhanced CH ₄ dissociation. | [189] |
| Rh-NiAl (1 wt.%/11.5 wt.%) Rh-Ni/Mg(Al)O (1.5 wt.%/12 wt.%) | Wet impregnation Support: Co-precipitation, Calcined at 800 °C for 3 h | GHSV = 22 L g ⁻¹ h ⁻¹ CH ₄ /CO ₂ = 1:1 T = 800 °C Max CH ₄ Conv. = 85% | - Samples promoted with Rh showed higher rates of carbon deposition compared to the non-promoted catalysts. | [190] |
| Ni-Fe/Mg(Al)O (8 wt.%/5 wt.%) (8 wt.%/8 wt.%) (8 wt.%/11 wt.%) | Incipient wetness impregnation; Support: Co-precipitation, Calcined at 750 °C for 4 h | GHSV = 166 L g ⁻¹ h ⁻¹ CH ₄ /CO ₂ = - T = 750 °C Max CH ₄ Conv. = NR | - Alloy composition and particle size depend on the homogeneous distribution of Ni and iron species during catalyst preparation. - Under low-temperature reforming conditions, the alloy Ni-Fe showed higher resistance to coke formation. | [191] |
| Ni-Fe/Mg(Al)O (8 wt.%/5 wt.%) | Incipient wetness impregnation; Support: Co-precipitation, Calcined: 750 °C for 4 h | GHSV = 30 L g ⁻¹ h ⁻¹ CH ₄ /CO ₂ = 1:1 T = 750 °C Max CH ₄ Conv. = NR | - CO ₂ regeneration led to the removal of carbon from the active metals of the catalysts. | [192] |
| Ni-Fe/Mg(Al)O (12 wt.%/3 wt.%) | Co-precipitation | GHSV = 60 L g ⁻¹ h ⁻¹ CH ₄ /CO ₂ = 1:1 T = 800 °C CH ₄ Conv. = 95% | - The catalyst showed good activity and stability in DRM at 500–800 °C. - Ni-Fe alloys can play different roles in DRM depending on the reaction conditions, especially at low reaction temperatures. | [193] |

⁽¹⁾ When not mentioned, reaction pressure is atmospheric; ⁽²⁾ Highest conversion reported among investigated catalysts; NR: not reported.

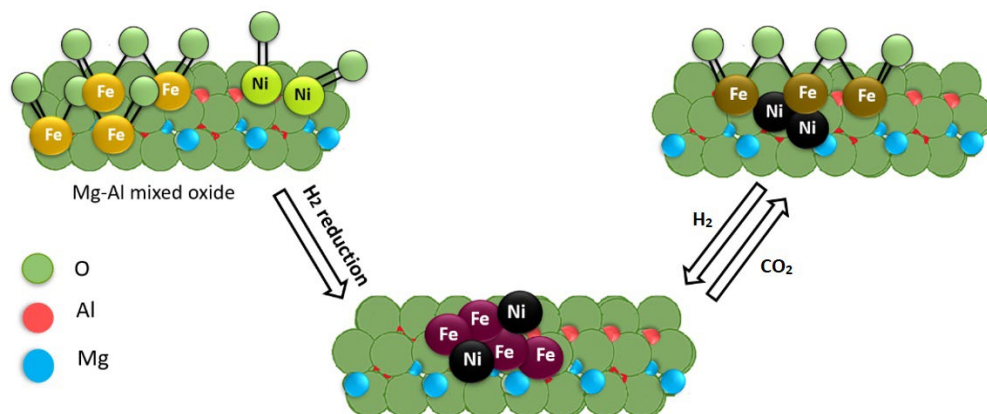


Figure 9. Schematic diagram of Fe-Ni alloy formation, during H₂ reduction, and decomposition, during CO₂ oxidation Adapted with permission from [191], copyright 2015, American Chemical Society.

Removal of carbon species from a Fe-Ni catalyst supported on Mg(Al)O after DRM at 750 °C was studied in another work by Theofanidis et al. [192]. The support material and the final catalyst were prepared by co-precipitation and incipient wetness impregnation methods, respectively. The elemental distribution of Fe-Ni proved that after CO₂ oxidation, segregation of Ni and Fe particles occurred as Fe was oxidized to Fe₃O₄, and the Fe-Ni alloy was decomposed. A subsequent H₂ reduction step could then lead back to Fe-Ni alloy and restore the original activity. It appears that in the process of carbon removal detected by XRD analyses and temporal analyses of the products, there were two parallel contributions: First the dissociation of CO₂ over Ni followed by oxidation of the carbon species by surface oxygen; second, the Fe oxidation by CO₂ followed by oxidation of carbon species by Fe oxide lattice oxygen (Fe oxide reduction step).

To study in more detail the effect of Fe addition, Wan et al. reduced a Ni-Fe/Mg(Al)O alloy catalyst at different temperatures [193]. The alloy catalyst was prepared by co-precipitation in one step and compared with Fe/Mg(Al)O and Ni/Mg(Al)O at the same metal content. Since CH₄ decomposition is an important reason for coking on Ni/Mg(Al)O, the activation energy of CH₄ was measured, indicating that the alloy Ni-Fe inhibited the CH₄ dissociation [86]. Compared with Ni-Fe/Al₂O₃ and Ni-Fe/Mg(Al)O catalysts prepared by the impregnation method, Ni-Fe alloy particles generated in situ from Mg(Ni, Fe, Al)O solid solutions yielded a catalyst with higher activity, stability, and good resistance to coking [194,195]. This can be attributed to the greater homogeneity of the alloy composition, which led to the formation of smaller particle sizes and stronger interaction of the metals with the support. It was proposed that CH₄ is mainly dissociated on the Ni sites forming adsorbed carbon, while CO₂ can provide adsorbed O through the activation at the metal-support sites to restore the active surface.

5. Conclusions and Perspectives

Ni/Mg(Al)O catalysts have been extensively studied in the last years due to their activity in both SMR and DRM reactions for H₂ production. What makes them so interesting is the possibility to finely tune their characteristics such as surface area, metal-support interaction, basicity, etc. by selecting the proper compositions, preparation methods, and thermal treatments. Here we summarized the most recent advances found in the literature about these catalysts, focusing on the strategies and their impact to enhance their catalytic activity and stability (Figure 10).

Ni/Mg(Al)O catalysts typically feature well-dispersed Ni metal particles (only up to about 15 wt.% Ni loadings) whose reducibility depends strongly on the composition and overall synthesis procedure [84,114]. NiO with little interaction with the support, for instance, may be exploited for low-temperature applications [196], while the formation of the Ni spinel phases with Al or Mg can suppress the Ni NPs sintering during high-temperature operations [55,56,60,61]. It is noteworthy that a certain amount of MgO was

found to be beneficial to limit the coke deposition due to its Lewis acidity [68]; an excessive loading, however, was reported to cause the failure of the catalyst [69].

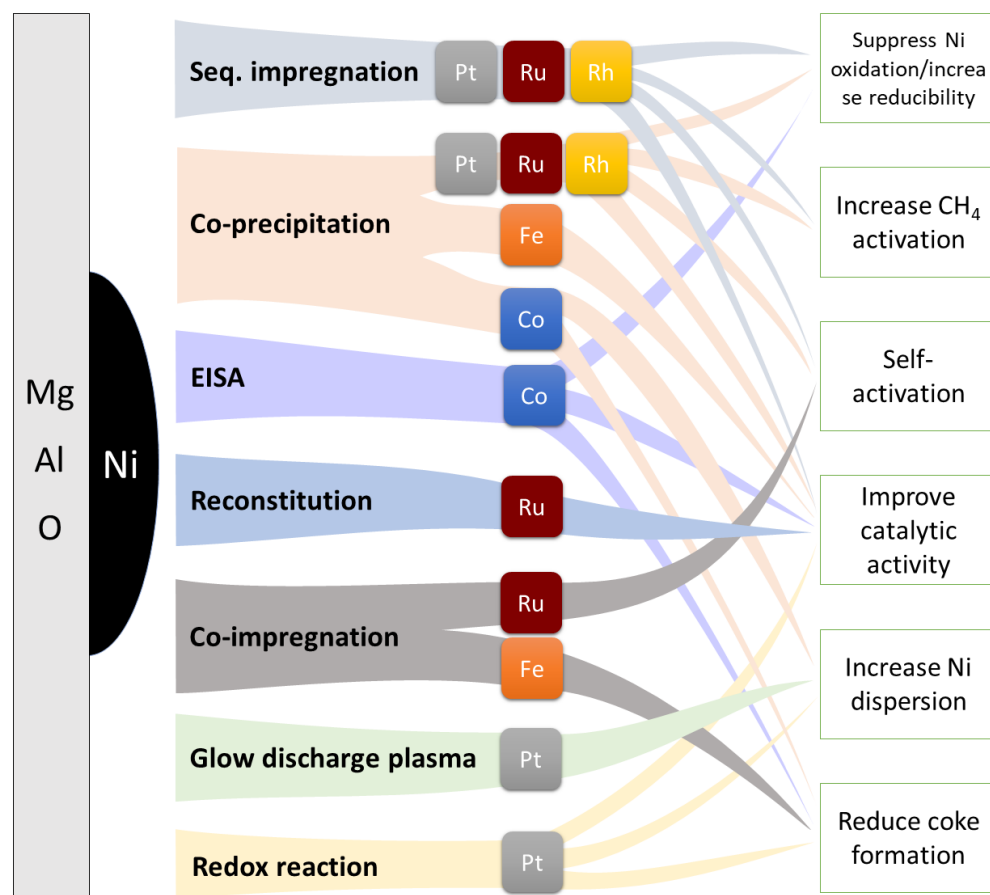


Figure 10. Schematic depiction of the main strategies adopted to enhance the catalytic activity of Ni-M/Mg(Al)O catalysts for SMR and DRM applications.

The monometallic Ni/Mg(Al)O catalysts, although very active in both reactions, suffer from Ni oxidation during daily start-up and shut-down operations [197]. Trace amounts of noble metal dopants such as Pt, Rh, and Ru easily suppress such oxidation and hence result in more stable catalysts. For SMR applications, only 0.1 wt.% of Pt or Rh added by the sequential impregnation method is enough to exert such a positive effect [145,146,151,153,198].

A remarkable feature of Ru-doped catalysts prepared by wet impregnation is that they are active without the need for reductive treatments prior to catalytic testing, which is an important economic point [157–159]. Not all noble metals are effective promoters though. A good example is Au, which showed a positive effect in retarding the coke formation in butane steam reforming [166]. In SMR, despite some modeling works predicting that alloying Au with Ni would hamper the coke formation [199,200], not only was it not completely suppressed, but the bimetallic Ni-Au catalysts were less active than the monometallic counterpart [166].

Apart from a recent work featuring Ni-Co catalysts prepared via a one-pot evaporation-induced self-assembly method with enhanced coke resistance [161], no promoting effects have been reported by adding non-noble metals to Ni/Mg(Al)O catalysts for SMR.

Pt, Ru, and Rh are among the most common promoters for Ni/Mg(Al)O catalysts for DRM. Once again, the main purpose of adding such metals is to increase the reducibility of Ni, but there are cases of Pt-modified materials, even in trimetallic formulations with Au [180], that show also a remarkably higher coke resistance [172,175,176,178,179]. Care must be paid as unwanted Ni segregation might occur while adding a noble metal promoter [190].

Contrary to SMR, there are few, but very interesting, examples of Ni catalysts promoted by non-noble metals. For example, Co, added by co-precipitation, can be exploited to control the metal–support interaction and in turn the size of Ni NPs. The resulting bimetallic catalysts showed enhanced stability in DRM [182]. A relevant coke deposition suppression effect was reported using Fe-Ni catalysts [191–193]. During the DRM reaction, the active phase is the Fe-Ni alloy, but some Fe oxide phases form and provide a surface O lattice that promotes coke gasification. Careful dosing of the two metals is critical to achieving this result [191,193,201].

To conclude, looking at Figure 10, two main considerations can be drawn about the attempts made at manufacturing highly performing and resistant Ni/Mg(Al)O catalysts for both CH₄ reforming processes. Firstly, co-precipitation is the most exploited synthetic method, likely because it has delivered the best results in terms of overall catalytic enhancements. The reason might be that having Ni within the main oxide matrix allows for finer control over the final Ni nanoparticles upon reduction treatments by regulating the metal–support interaction [54,86,161]. Secondly, there is still an overdependence on noble metals as too few base metals have shown sufficient promoting effects. Fe is a promising candidate, but only in DRM, whereas it catastrophically oxidizes during SMR leading to inactive Fe oxide phases [202]. So far, no active Ni-Fe catalysts have been reported for SMR. This hints at the fact that despite sharing many similarities, SMR and DRM reactions are too different to have a catalyst active and stable in both, hence the development of new catalysts should be tailored to the specific reaction.

It is evident from this literature review that some challenges remain for Ni/Mg(Al)O catalysts for SMR and DRM applications. Probably the most crucial is the tendency of Ni to oxidize under the harsh reaction conditions typical of both processes. So far, only noble metals have proved effective in suppressing that, which makes the development of non-noble promoters for SMR even more urgent. Moreover, considering the sensitivity of both the processes to the Ni NPs size, what appears from the literature is that there is still a rather poor control over the final NPs sizes, especially for high temperatures and long-run applications. In addition, while both Mg and Al are necessary to achieve high activity and stability, there is also a lack of control over the final location of the Ni NPs upon reduction, meaning that it is hard to control with which crystal phase the Ni NPs preferentially interact.

Another important factor affecting both reactions is the coke resistance. Again, in SMR, essentially only noble metals can suppress the coke deposition.

What is really lacking in the study and development of Ni(M)/MgAlO catalysts for both SMR and DRM reactions is a deep understanding of the catalysts under working conditions. There are some examples of investigations carried out in operando or in-situ conditions, but they are mostly XRD [119,182] and DRIFTS [144] focused on revealing the crystal phases after reduction and the Ni-Ru interaction, respectively. Others studied the basicity of the catalysts after reductive treatments via CO₂-TPD analyses [140] and the Ni NPs' growth after steam treatments through HRTEM [154]. More detailed studies evidencing the transformations occurring during the reductive treatments and during the catalytic reactions, perhaps focusing on the electronic and actual metal–support interaction, are needed.

One strategy worth pursuing to prepare more active Ni(M)/MgAlO catalysts might consist in better exploiting the phase composition of the Mg-Al-O supports. An effective way to prepare catalysts featuring the correct amounts of MgO and NiO-MgO phases—which improve, respectively, the coke resistance and prevent the Ni NPs sintering upon reduction—is needed, possibly through the memory effect of hydrotalcite materials. More advanced preparation methods, such as ALD, have allowed a deeper understanding as well as finer control over many parameters affecting the final catalytic activity but seem hard to scale up. Some methods to prepare catalysts in large quantities (such as kneading) and already in a suitable shape for large-scale reactors (such as 3D printing) have been patented, but are limited to monometallic formulations for SMR while bimetallic catalysts are reported to show improved coke resistance only when using simulated natural gas, which is, in other words, during the DRM reaction.

Author Contributions: Conceptualization, F.B., C.E. and V.D.S.; writing—original draft preparation, S.S. and X.T.N.; writing—review and editing, F.B., C.E. and V.D.S.; supervision, C.E. and V.D.S.; funding acquisition, C.E. and V.D.S. All authors have read and agreed to the published version of the manuscript.

Funding: The authors thank the financial support through the BIKE project; this project has received funding from the European Union’s Horizon 2020 research and innovation program under the Marie Skłodowska-Curie grant agreement No. 813748.

Data Availability Statement: No new data were created or analyzed in this study. Data sharing is not applicable to this article.

Conflicts of Interest: There are no conflicts to declare.

References

1. European Commission. Directorate General for Research and Innovation. In *Horizon Europe: Strategic Plan 2021–2024*; Publications Office: Luxembourg, 2021.
2. Chen, L.; Qi, Z.; Zhang, S.; Su, J.; Somorjai, G.A. Catalytic Hydrogen Production from Methane: A Review on Recent Progress and Prospect. *Catalysts* **2020**, *10*, 858. [[CrossRef](#)]
3. Iulianelli, A.; Liguori, S.; Wilcox, J.; Basile, A. Advances on Methane Steam Reforming to Produce Hydrogen through Membrane Reactors Technology: A Review. *Catal. Rev.* **2016**, *58*, 1–35. [[CrossRef](#)]
4. Lavoie, J.M. Review on Dry Reforming of Methane, a Potentially More Environmentally Friendly Approach to the Increasing Natural Gas Exploitation. *Front. Chem.* **2014**, *2*, 81. [[CrossRef](#)]
5. Jang, W.-J.; Shim, J.-O.; Kim, H.-M.; Yoo, S.-Y.; Roh, H.-S. A Review on Dry Reforming of Methane in Aspect of Catalytic Properties. *Catal. Today* **2019**, *324*, 15–26. [[CrossRef](#)]
6. Pakhare, D.; Spivey, J. A Review of Dry (CO₂) Reforming of Methane over Noble Metal Catalysts. *Chem. Soc. Rev.* **2014**, *43*, 7813–7837. [[CrossRef](#)]
7. Ismagilov, Z.R.; Matus, E.V.; Ismagilov, I.Z.; Sukhova, O.B.; Yashnik, S.A.; Ushakov, V.A.; Kerzhentsev, M.A. Hydrogen Production through Hydrocarbon Fuel Reforming Processes over Ni Based Catalysts. *Catal. Today* **2019**, *323*, 166–182. [[CrossRef](#)]
8. Armor, J.N. The Multiple Roles for Catalysis in the Production of H₂. *Appl. Catal. A Gen.* **1999**, *176*, 159–176. [[CrossRef](#)]
9. Joensen, F.; Rostrup-Nielsen, J.R. Conversion of Hydrocarbons and Alcohols for Fuel Cells. *J. Power Sources* **2002**, *105*, 195–201. [[CrossRef](#)]
10. Kalamaras, C.M.; Efstathiou, A.M. Hydrogen Production Technologies: Current State and Future Developments. *Conf. Pap. Energy* **2013**, *2013*, 690627. [[CrossRef](#)]
11. Kulkarni, S. A Review on Reforming Reactions with Emphasis on Methane Reforming. *Int. J. Res. Rev.* **2016**, *3*, 20–23.
12. Chai, S.; Zhang, G.; Li, G.; Zhang, Y. Industrial Hydrogen Production Technology and Development Status in China: A Review. *Clean Technol. Environ. Policy* **2021**, *23*, 1931–1946. [[CrossRef](#)]
13. Nikoo, M.K.; Amin, N.A.S. Thermodynamic Analysis of Carbon Dioxide Reforming of Methane in View of Solid Carbon Formation. *Fuel Process. Technol.* **2011**, *92*, 678–691. [[CrossRef](#)]
14. Özkara-Aydinoğlu, Ş.; Aksoylu, A.E. CO₂ Reforming of Methane over Pt–Ni/Al₂O₃ Catalysts: Effects of Catalyst Composition, and Water and Oxygen Addition to the Feed. *Int. J. Hydrogen Energy* **2011**, *36*, 2950–2959. [[CrossRef](#)]
15. Kim, H.Y.; Park, J.-N.; Henkelman, G.; Kim, J.M. Design of a Highly Nanodispersed Pd–MgO/SiO₂ Composite Catalyst with Multifunctional Activity for CH₄ Reforming. *ChemSusChem* **2012**, *5*, 1474–1481. [[CrossRef](#)] [[PubMed](#)]
16. Bradford, M.C.J.; Vannice, M.A. CO₂ Reforming of CH₄. *Catal. Rev.* **1999**, *41*, 1–42. [[CrossRef](#)]
17. Mondal, K.; Sasmal, S.; Badgandi, S.; Chowdhury, D.R.; Nair, V. Dry Reforming of Methane to Syngas: A Potential Alternative Process for Value Added Chemicals—A Techno-Economic Perspective. *Environ. Sci. Pollut. Res.* **2016**, *23*, 22267–22273. [[CrossRef](#)]
18. Parsapur, R.K.; Chatterjee, S.; Huang, K.-W. The Insignificant Role of Dry Reforming of Methane in CO₂ Emission Relief. *ACS Energy Lett.* **2020**, *5*, 2881–2885. [[CrossRef](#)]
19. Noureldin, M.M.B.; Elbasher, N.O.; Gabriel, K.J.; El-Halwagi, M.M. A Process Integration Approach to the Assessment of CO₂ Fixation through Dry Reforming. *ACS Sustain. Chem. Eng.* **2015**, *3*, 625–636. [[CrossRef](#)]
20. Cai, X.; Hu, Y.H. Advances in Catalytic Conversion of Methane and Carbon Dioxide to Highly Valuable Products. *Energy Sci. Eng.* **2019**, *7*, 4–29. [[CrossRef](#)]
21. Rostrup-Nielsen, J.R.; Sehested, J.; Nørskov, J.K. Hydrogen and Synthesis Gas by Steam-and CO₂ Reforming. *Adv. Catal.* **2002**, *47*, 65–139. [[CrossRef](#)]
22. Rostrup-Nielsen, J.; Christiansen, L.J. Concepts in Syngas Manufacture. *Catal. Sci. Ser.* **2011**, *10*, 392. [[CrossRef](#)]
23. Rostrup-Nielsen, J.R.; Hansen, J.H.B. CO₂-Reforming of Methane over Transition Metals. *J. Catal.* **1993**, *144*, 38–49. [[CrossRef](#)]
24. Jones, G.; Jakobsen, J.G.; Shim, S.S.; Kleis, J.; Andersson, M.P.; Rossmeisl, J.; Abild-Pedersen, F.; Bligaard, T.; Helveg, S.; Hinnemann, B.; et al. First Principles Calculations and Experimental Insight into Methane Steam Reforming over Transition Metal Catalysts. *J. Catal.* **2008**, *259*, 147–160. [[CrossRef](#)]
25. Wu, H.; La Parola, V.; Pantaleo, G.; Puleo, F.; Venezia, A.; Liotta, L. Ni-Based Catalysts for Low Temperature Methane Steam Reforming: Recent Results on Ni–Au and Comparison with Other Bi-Metallic Systems. *Catalysts* **2013**, *3*, 563–583. [[CrossRef](#)]

26. De, S.; Zhang, J.; Luque, R.; Yan, N. Ni-Based Bimetallic Heterogeneous Catalysts for Energy and Environmental Applications. *Energy Environ. Sci.* **2016**, *9*, 3314–3347. [[CrossRef](#)]
27. Trimm, D.L. Coke Formation and Minimisation during Steam Reforming Reactions. *Catal. Today* **1997**, *37*, 233–238. [[CrossRef](#)]
28. Trimm, D.L. Catalysts for the Control of Coking during Steam Reforming. *Catal. Today* **1999**, *49*, 3–10. [[CrossRef](#)]
29. Sehested, J. Four Challenges for Nickel Steam-Reforming Catalysts. *Catal. Today* **2006**, *111*, 103–110. [[CrossRef](#)]
30. Theofanidis, S.A.; Galvita, V.V.; Poelman, H.; Batchu, R.; Buelens, L.C.; Detavernier, C.; Marin, G.B. Mechanism of Carbon Deposits Removal from Supported Ni Catalysts. *Appl. Catal. B Environ.* **2018**, *239*, 502–512. [[CrossRef](#)]
31. Li, D.; Nakagawa, Y.; Tomishige, K. Methane Reforming to Synthesis Gas over Ni Catalysts Modified with Noble Metals. *Appl. Catal. A Gen.* **2011**, *408*, 1–24. [[CrossRef](#)]
32. Roussière, T.; Schulz, L.; Schelkle, K.M.; Wasserschaff, G.; Milanov, A.; Schwab, E.; Deutschmann, O.; Jentys, A.; Lercher, J.; Schunk, S.A. Structure–Activity Relationships of Nickel–Hexaaluminates in Reforming Reactions Part II: Activity and Stability of Nanostructured Nickel–Hexaaluminate-Based Catalysts in the Dry Reforming of Methane. *ChemCatChem* **2014**, *6*, 1447–1452. [[CrossRef](#)]
33. Ginsburg, J.M.; Piña, J.; El Solh, T.; de Lasa, H.I. Coke Formation over a Nickel Catalyst under Methane Dry Reforming Conditions: Thermodynamic and Kinetic Models. *Ind. Eng. Chem. Res.* **2005**, *44*, 4846–4854. [[CrossRef](#)]
34. Titus, J.; Roussière, T.; Wasserschaff, G.; Schunk, S.; Milanov, A.; Schwab, E.; Wagner, G.; Oeckler, O.; Gläser, R. Dry Reforming of Methane with Carbon Dioxide over NiO–MgO–ZrO₂. *Catal. Today* **2016**, *270*, 68–75. [[CrossRef](#)]
35. Aramouni, N.A.K.; Touma, J.G.; Tarboush, B.A.; Zeaiter, J.; Ahmad, M.N. Catalyst Design for Dry Reforming of Methane: Analysis Review. *Renew. Sustain. Energy Rev.* **2018**, *82*, 2570–2585. [[CrossRef](#)]
36. Van Hook, J.P. Methane-Steam Reforming. *Catal. Rev.* **1980**, *21*, 1–51. [[CrossRef](#)]
37. Hu, Y.H. Advances in Catalysts for CO₂ Reforming of Methane. In *Advances in CO₂ Conversion and Utilization*; American Chemical Society: Washington, DC, USA, 2010; pp. 155–174.
38. Lee, S. *Methane and Its Derivatives*; CRC Press: Boca Raton, FL, USA, 2017.
39. Hu, Y.H.; Ruckenstein, E. Binary MgO-Based Solid Solution Catalysts for Methane Conversion to Syngas. *Catal. Rev.* **2002**, *44*, 423–453. [[CrossRef](#)]
40. Fan, M.-S.; Abdullah, A.Z.; Bhatia, S. Catalytic Technology for Carbon Dioxide Reforming of Methane to Synthesis Gas. *ChemCatChem* **2009**, *1*, 192–208. [[CrossRef](#)]
41. Muraza, O.; Galadima, A. A Review on Coke Management during Dry Reforming of Methane. *Int. J. Energy Res.* **2015**, *39*, 1196–1216. [[CrossRef](#)]
42. Arora, S.; Prasad, R. An Overview on Dry Reforming of Methane: Strategies to Reduce Carbonaceous Deactivation of Catalysts. *RSC Adv.* **2016**, *6*, 108668–108688. [[CrossRef](#)]
43. Guo, J.; Lou, H.; Zhao, H.; Chai, D.; Zheng, X. Dry Reforming of Methane over Nickel Catalysts Supported on Magnesium Aluminate Spinels. *Appl. Catal. A Gen.* **2004**, *273*, 75–82. [[CrossRef](#)]
44. Alonso, D.M.; Wettstein, S.G.; Dumesic, J.A. Bimetallic Catalysts for Upgrading of Biomass to Fuels and Chemicals. *Chem. Soc. Rev.* **2012**, *41*, 8075–8098. [[CrossRef](#)] [[PubMed](#)]
45. Dal Santo, V.; Gallo, A.; Naldoni, A.; Guidotti, M.; Psaro, R. Bimetallic Heterogeneous Catalysts for Hydrogen Production. *Catal. Today* **2012**, *197*, 190–205. [[CrossRef](#)]
46. Usman, M.; Daud, W.W.; Abbas, H.F. Dry Reforming of Methane: Influence of Process Parameters—A Review. *Renew. Sustain. Energy Rev.* **2015**, *45*, 710–744. [[CrossRef](#)]
47. Puxley, D.C.; Kitchener, I.J.; Komodromos, C.; Parkyns, N.D. The Effect Of Preparation Method Upon The Structures, Stability And Metal/Support Interactions In Nickel/Alumina Catalysts. In *Studies in Surface Science and Catalysis*; Poncelet, G., Grange, P., Jacobs, P.A., Eds.; Elsevier: Amsterdam, The Netherlands, 1983; Volume 16, pp. 237–271.
48. Azancot, L.; Bobadilla, L.F.; Santos, J.L.; Córdoba, J.M.; Centeno, M.A.; Odriozola, J.A. Influence of the Preparation Method in the Metal-Support Interaction and Reducibility of Ni-Mg-Al Based Catalysts for Methane Steam Reforming. *Int. J. Hydrogen Energy* **2019**, *44*, 19827–19840. [[CrossRef](#)]
49. Kwon, D.; Kang, J.Y.; An, S.; Yang, I.; Jung, J.C. Tuning the Base Properties of Mg–Al Hydrotalcite Catalysts Using Their Memory Effect. *J. Energy Chem.* **2020**, *46*, 229–236. [[CrossRef](#)]
50. Bossola, F.; Evangelisti, C.; Allieta, M.; Psaro, R.; Recchia, S.; Dal Santo, V. Well-Formed, Size-Controlled Ruthenium Nanoparticles Active and Stable for Acetic Acid Steam Reforming. *Appl. Catal. B Environ.* **2016**, *181*, 599–611. [[CrossRef](#)]
51. Adamu, S.; Bawah, A.-R.; Muraza, O.; Malaibari, Z.; Hossain, M.M. Effects of Metal Support Interaction on Dry Reforming of Methane over Ni/Ce–Al₂O₃ Catalysts. *Can. J. Chem. Eng.* **2020**, *98*, 2425–2434. [[CrossRef](#)]
52. Kumar, R.; Kumar, K.; Pant, K.K.; Choudary, N.V. Tuning the Metal-Support Interaction of Methane Tri-Reforming Catalysts for Industrial Flue Gas Utilization. *Int. J. Hydrogen Energy* **2020**, *45*, 1911–1929. [[CrossRef](#)]
53. Özdemir, H.; Öksüzömer, M.A.F.; Gürkaynak, M.A. Effect of the Calcination Temperature on Ni/MgAl₂O₄ Catalyst Structure and Catalytic Properties for Partial Oxidation of Methane. *Fuel* **2014**, *116*, 63–70. [[CrossRef](#)]
54. Li, C.; Chen, Y.-W. Temperature-Programmed-Reduction Studies of Nickel Oxide/Alumina Catalysts: Effects of the Preparation Method. *Thermochim. Acta* **1995**, *256*, 457–465. [[CrossRef](#)]
55. Rynkowski, J.M.; Paryjczak, T.; Lenik, M. On the Nature of Oxidic Nickel Phases in NiO/γ-Al₂O₃ Catalysts. *Appl. Catal. A Gen.* **1993**, *106*, 73–82. [[CrossRef](#)]

56. Zhang, C.; Hu, X.; Zhang, Z.; Zhang, L.; Dong, D.; Gao, G.; Westerhof, R.; Syed-Hassan, S.S.A. Steam Reforming of Acetic Acid over Ni/Al₂O₃ Catalyst: Correlation of Calcination Temperature with the Interaction of Nickel and Alumina. *Fuel* **2018**, *227*, 307–324. [CrossRef]
57. Sahli, N.; Petit, C.; Roger, A.-C.; Kiennemann, A.; Libs, S.; Bettahar, M.M. Ni Catalysts from NiAl₂O₄ Spinel for CO₂ Reforming of Methane. *Catal. Today* **2006**, *113*, 187–193. [CrossRef]
58. Kuzmin, A.; Mironova, N. Composition Dependence of the Lattice Parameter in Solid Solutions. *J. Phys. Matter* **1998**, *10*, 7937–7944. [CrossRef]
59. Parmaliana, A.; Arena, F.; Frusteri, F.; Giordano, N. Temperature-Programmed Reduction Study of NiO–MgO Interactions in Magnesia-Supported Ni Catalysts and NiO–MgO Physical Mixture. *J. Chem. Soc. Faraday Trans.* **1990**, *86*, 2663–2669. [CrossRef]
60. Zanganeh, R.; Rezaei, M.; Zamaniyan, A. Dry Reforming of Methane to Synthesis Gas on NiO–MgO Nanocrystalline Solid Solution Catalysts. *Int. J. Hydrogen Energy* **2013**, *38*, 3012–3018. [CrossRef]
61. Ruckenstein, E.; Hu, Y.H. Carbon Dioxide Reforming of Methane over Nickel/Alkaline Earth Metal Oxide Catalysts. *Appl. Catal. A Gen.* **1995**, *133*, 149–161. [CrossRef]
62. Ou, Z.; Zhang, Z.; Qin, C.; Xia, H.; Deng, T.; Niu, J.; Ran, J.; Wu, C. Highly Active and Stable Ni/Perovskite Catalysts in Steam Methane Reforming for Hydrogen Production. *Sustain. Energy Fuels* **2021**, *5*, 1845–1856. [CrossRef]
63. Hong Phuong, P.; Cam Anh, H.; Tri, N.; Phung Anh, N.; Cam Loc, L. Effect of Support on Stability and Coke Resistance of Ni-Based Catalyst in Combined Steam and CO₂ Reforming of CH₄. *ACS Omega* **2022**, *7*, 20092–20103. [CrossRef]
64. Gac, W. Acid–Base Properties of Ni–MgO–Al₂O₃ Materials. *Appl. Surf. Sci.* **2011**, *257*, 2875–2880. [CrossRef]
65. Coleman, L.J.I.; Epling, W.; Hudgins, R.R.; Croiset, E. Ni/Mg–Al Mixed Oxide Catalyst for the Steam Reforming of Ethanol. *Appl. Catal. A Gen.* **2009**, *363*, 52–63. [CrossRef]
66. Damyanova, S.; Pawelec, B.; Arishtirova, K.; Fierro, J.L.G. Ni-Based Catalysts for Reforming of Methane with CO₂. *Int. J. Hydrogen Energy* **2012**, *37*, 15966–15975. [CrossRef]
67. Zhang, R.; Xia, G.; Li, M.; Wu, Y.; Nie, H.; Li, D. Effect of Support on the Performance of Ni-Based Catalyst in Methane Dry Reforming. *J. Fuel Chem. Technol.* **2015**, *43*, 1359–1365. [CrossRef]
68. Mehr, J.Y.; Jozani, K.J.; Pour, A.N.; Zamani, Y. Influence of MgO in the CO₂–Steam Reforming of Methane to Syngas by NiO/MgO/α-Al₂O₃ Catalyst. *React. Kinet. Catal. Lett.* **2002**, *75*, 267–273. [CrossRef]
69. Das, S.; Sengupta, M.; Patel, J.; Bordoloi, A. A Study of the Synergy between Support Surface Properties and Catalyst Deactivation for CO₂ Reforming over Supported Ni Nanoparticles. *Appl. Catal. A Gen.* **2017**, *545*, 113–126. [CrossRef]
70. Williams, G.R.; O’Hare, D. Towards Understanding, Control and Application of Layered Double Hydroxide Chemistry. *J. Mater. Chem.* **2006**, *16*, 3065–3074. [CrossRef]
71. Cavani, F.; Trifirò, F.; Vaccari, A. Hydrotalcite-Type Anionic Clays: Preparation, Properties and Applications. *Catal. Today* **1991**, *11*, 173–301. [CrossRef]
72. Sikander, U.; Sufian, S.; Salam, M.A. A Review of Hydrotalcite Based Catalysts for Hydrogen Production Systems. *Int. J. Hydrogen Energy* **2017**, *42*, 19851–19868. [CrossRef]
73. Debek, R.; Motak, M.; Grzybek, T.; Galvez, M.E.; Da Costa, P. A Short Review on the Catalytic Activity of Hydrotalcite-Derived Materials for Dry Reforming of Methane. *Catalysts* **2017**, *7*, 32. [CrossRef]
74. Bhattacharyya, A.; Chang, V.W.; Schumacher, D.J. CO₂ Reforming of Methane to Syngas: I: Evaluation of Hydrotalcite Clay-Derived Catalysts. *Appl. Clay Sci.* **1998**, *13*, 317–328. [CrossRef]
75. Fornasari, G.; Gazzano, M.; Matteuzzi, D.; Trifirò, F.; Vaccari, A. Structure and Reactivity of High-Surface-Area Ni/Mg/Al Mixed Oxides. *Appl. Clay Sci.* **1995**, *10*, 69–82. [CrossRef]
76. Shishido, T.; Sukenobu, M.; Morioka, H.; Kondo, M.; Wang, Y.; Takaki, K.; Takehira, K. Partial Oxidation of Methane over Ni/Mg–Al Oxide Catalysts Prepared by Solid Phase Crystallization Method from Mg–Al Hydrotalcite-like Precursors. *Appl. Catal. A Gen.* **2002**, *223*, 35–42. [CrossRef]
77. Shishido, T.; Wang, P.; Kosaka, T.; Takehira, K. Steam Reforming of CH₄ over Ni/Mg–Al Catalyst Prepared by Spc-Method from Hydrotalcite. *Chem. Lett.* **2002**, *31*, 752–753. [CrossRef]
78. Di Cosimo, J.I.; Díez, V.K.; Xu, M.; Iglesia, E.; Apesteguía, C.R. Structure and Surface and Catalytic Properties of Mg–Al Basic Oxides. *J. Catal.* **1998**, *178*, 499–510. [CrossRef]
79. Takehira, K.; Shishido, T.; Wang, P.; Kosaka, T.; Takaki, K. Steam Reforming of CH₄ over Supported Ni Catalysts Prepared from a Mg–Al Hydrotalcite-like Anionic Clay. *Phys. Chem. Chem. Phys.* **2003**, *5*, 3801–3810. [CrossRef]
80. Shishido, T.; Sukenobu, M.; Morioka, H.; Furukawa, R.; Shirahase, H.; Takehira, K. CO₂ Reforming of CH₄ over Ni/Mg–Al Oxide Catalysts Prepared by Solid Phase Crystallization Method from Mg–Al Hydrotalcite-like Precursors. *Catal. Lett.* **2001**, *73*, 21–26. [CrossRef]
81. Mehrabadi, B.A.T.; Eskandari, S.; Khan, U.; White, R.D.; Regalbutto, J.R. Chapter One—A Review of Preparation Methods for Supported Metal Catalysts. In *Advances in Catalysis*; Song, C., Ed.; Academic Press: Cambridge, MA, USA, 2017; Volume 61, pp. 1–35.
82. Touahra, F.; Sehaïlia, M.; Ketir, W.; Bachari, K.; Chebout, R.; Trari, M.; Cherifi, O.; Halliche, D. Effect of the Ni/Al Ratio of Hydrotalcite-Type Catalysts on Their Performance in the Methane Dry Reforming Process. *Appl. Petrochem. Res.* **2016**, *6*, 1–13. [CrossRef]
83. Li, L.; Zhang, L.; Zhang, Y.; Li, J. Effect of Ni Loadings on the Catalytic Properties of Ni/MgO(111) Catalyst for the Reforming of Methane with Carbon Dioxide. *J. Fuel Chem. Technol.* **2015**, *43*, 315–322. [CrossRef]

84. Alipour, Z.; Rezaei, M.; Meshkani, F. Effect of Ni Loadings on the Activity and Coke Formation of MgO-Modified Ni/Al₂O₃ Nanocatalyst in Dry Reforming of Methane. *J. Energy Chem.* **2014**, *23*, 633–638. [[CrossRef](#)]
85. Akbari, E.; Alavi, S.M.; Rezaei, M. Synthesis Gas Production over Highly Active and Stable Nanostructured Ni-MgO-Al₂O₃ Catalysts in Dry Reforming of Methane: Effects of Ni Contents. *Fuel* **2017**, *194*, 171–179. [[CrossRef](#)]
86. Debek, R.; Motak, M.; Duraczyska, D.; Launay, F.; Galvez, M.E.; Grzybek, T.; Da Costa, P. Methane Dry Reforming over Hydrotalcite-Derived Ni-Mg-Al Mixed Oxides: The Influence of Ni Content on Catalytic Activity, Selectivity and Stability. *Catal. Sci. Technol.* **2016**, *6*, 6705–6715. [[CrossRef](#)]
87. Lin, X.; Li, R.; Lu, M.; Chen, C.; Li, D.; Zhan, Y.; Jiang, L. Carbon Dioxide Reforming of Methane over Ni Catalysts Prepared from Ni-Mg-Al Layered Double Hydroxides: Influence of Ni Loadings. *Fuel* **2015**, *162*, 271–280. [[CrossRef](#)]
88. Qi, Y.; Cheng, Z.; Zhou, Z. Steam Reforming of Methane over Ni Catalysts Prepared from Hydrotalcite-Type Precursors: Catalytic Activity and Reaction Kinetics. *Chin. J. Chem. Eng.* **2015**, *23*, 76–85. [[CrossRef](#)]
89. Bian, Z.; Zhong, W.; Yu, Y.; Wang, Z.; Jiang, B.; Kawi, S. Dry Reforming of Methane on Ni/Mesoporous-Al₂O₃ Catalysts: Effect of Calcination Temperature. *Int. J. Hydrogen Energy* **2021**, *46*, 31041–31053. [[CrossRef](#)]
90. Al-Fatesh, A.S.A.; Fakeeha, A.H. Effects of Calcination and Activation Temperature on Dry Reforming Catalysts. *J. Saudi Chem. Soc.* **2012**, *16*, 55–61. [[CrossRef](#)]
91. Juan-Juan, J.; Román-Martínez, M.C.; Illán-Gómez, M.J. Nickel Catalyst Activation in the Carbon Dioxide Reforming of Methane: Effect of Pretreatments. *Appl. Catal. A Gen.* **2009**, *355*, 27–32. [[CrossRef](#)]
92. Zhou, L.; Li, L.; Wei, N.; Li, J.; Basset, J.-M. Effect of NiAl₂O₄ Formation on Ni/Al₂O₃ Stability during Dry Reforming of Methane. *ChemCatChem* **2015**, *7*, 2508–2516. [[CrossRef](#)]
93. Feng, J.; Ding, Y.; Guo, Y.; Li, X.; Li, W. Calcination Temperature Effect on the Adsorption and Hydrogenated Dissociation of CO₂ over the NiO/MgO Catalyst. *Fuel* **2013**, *109*, 110–115. [[CrossRef](#)]
94. Ruckenstein, E.; Hang Hu, Y. The Effect of Precursor and Preparation Conditions of MgO on the CO₂ Reforming of CH₄ over NiO/MgO Catalysts. *Appl. Catal. A Gen.* **1997**, *154*, 185–205. [[CrossRef](#)]
95. Mette, K.; Kühn, S.; Düdler, H.; Kähler, K.; Tarasov, A.; Muhler, M.; Behrens, M. Stable Performance of Ni Catalysts in the Dry Reforming of Methane at High Temperatures for the Efficient Conversion of CO₂ into Syngas. *ChemCatChem* **2014**, *6*, 100–104. [[CrossRef](#)]
96. Katheria, S.; Gupta, A.; Deo, G.; Kunzru, D. Effect of Calcination Temperature on Stability and Activity of Ni/MgAl₂O₄ Catalyst for Steam Reforming of Methane at High Pressure Condition. *Int. J. Hydrogen Energy* **2016**, *41*, 14123–14132. [[CrossRef](#)]
97. Li, X.; Huang, Y.; Zhang, Q.; Luan, C.; Vinokurov, V.A.; Huang, W. Highly Stable and Anti-Coking Ni/MoCeZr/MgAl₂O₄-MgO Complex Support Catalysts for CO₂ Reforming of CH₄: Effect of the Calcination Temperature. *Energy Convers. Manag.* **2019**, *179*, 166–177. [[CrossRef](#)]
98. Perez-Lopez, O.W.; Senger, A.; Marcilio, N.R.; Lansarin, M.A. Effect of Composition and Thermal Pretreatment on Properties of Ni-Mg-Al Catalysts for CO₂ Reforming of Methane. *Appl. Catal. A Gen.* **2006**, *303*, 234–244. [[CrossRef](#)]
99. Djaidja, A.; Libs, S.; Kiennemann, A.; Barama, A. Characterization and Activity in Dry Reforming of Methane on NiMg/Al and Ni/MgO Catalysts. *Catal. Today* **2006**, *113*, 194–200. [[CrossRef](#)]
100. Wang, Y.; Wang, H.; Dam, A.H.; Xiao, L.; Qi, Y.; Niu, J.; Yang, J.; Zhu, Y.-A.; Holmen, A.; Chen, D. Understanding Effects of Ni Particle Size on Steam Methane Reforming Activity by Combined Experimental and Theoretical Analysis. *Catal. Today* **2019**, *355*, 139–147. [[CrossRef](#)]
101. Kim, J.-H.; Suh, D.J.; Park, T.-J.; Kim, K.-L. Effect of Metal Particle Size on Coking during CO₂ Reforming of CH₄ over Ni-Alumina Aerogel Catalysts. *Appl. Catal. A Gen.* **2000**, *197*, 191–200. [[CrossRef](#)]
102. Vogt, C.; Kranenborg, J.; Monai, M.; Weckhuysen, B.M. Structure Sensitivity in Steam and Dry Methane Reforming over Nickel: Activity and Carbon Formation. *ACS Catal.* **2020**, *10*, 1428–1438. [[CrossRef](#)]
103. Munnik, P.; de Jongh, P.E.; de Jong, K.P. Recent Developments in the Synthesis of Supported Catalysts. *Chem. Rev.* **2015**, *115*, 6687–6718. [[CrossRef](#)]
104. Roh, H.-S.; Eum, I.-H.; Jeong, D.-W.; Yi, B.E.; Na, J.-G.; Ko, C.H. The Effect of Calcination Temperature on the Performance of Ni/MgO-Al₂O₃ Catalysts for Decarboxylation of Oleic Acid. *Catal. Today* **2011**, *164*, 457–460. [[CrossRef](#)]
105. Smoláková, L.; Kout, M.; Koudelková, E.; Čapek, L. Effect of Calcination Temperature on the Structure and Catalytic Performance of the Ni/Al₂O₃ and Ni-Ce/Al₂O₃ Catalysts in Oxidative Dehydrogenation of Ethane. *Ind. Eng. Chem. Res.* **2015**, *54*, 12730–12740. [[CrossRef](#)]
106. Khan, A.I.; O'Hare, D. Intercalation Chemistry of Layered Double Hydroxides: Recent Developments and Applications. *J. Mater. Chem.* **2002**, *12*, 3191–3198. [[CrossRef](#)]
107. Millet, M.-M.; Tarasov, A.V.; Girgsdies, F.; Algara-Siller, G.; Schlögl, R.; Frei, E. Highly Dispersed Ni₀/Ni_xMg_{1-x}O Catalysts Derived from Solid Solutions: How Metal and Support Control the CO₂ Hydrogenation. *ACS Catal.* **2019**, *9*, 8534–8546. [[CrossRef](#)]
108. Ward, D.A.; Ko, E.I. Preparing Catalytic Materials by the Sol-Gel Method. *Ind. Eng. Chem. Res.* **1995**, *34*, 421–433. [[CrossRef](#)]
109. Frenzer, G.; Maier, W.F. Amorphous Porous Mixed Oxides: Sol-Gel Ways to a Highly Versatile Class of Materials and Catalysts. *Annu. Rev. Mater. Res.* **2006**, *36*, 281–331. [[CrossRef](#)]
110. Othman, M.R.; Helwani, Z.; Martunus; Fernando, W.J.N. Synthetic Hydrotalcites from Different Routes and Their Application as Catalysts and Gas Adsorbents: A Review. *Appl. Organomet. Chem.* **2009**, *23*, 335–346. [[CrossRef](#)]

111. Miller, J.B.; Ko, E.I. Control of Mixed Oxide Textural and Acidic Properties by the Sol-Gel Method. *Catal. Today* **1997**, *35*, 269–292. [[CrossRef](#)]
112. Otero Areán, C.; Peñarroya Mentrut, M.; López López, A.J.; Parra, J.B. High Surface Area Nickel Aluminate Spinel Prepared by a Sol-Gel Method. *Colloids Surf. A Physicochem. Eng. Asp.* **2001**, *180*, 253–258. [[CrossRef](#)]
113. Li, H.; Xu, H.; Wang, J. Methane Reforming with CO₂ to Syngas over CeO₂-Promoted Ni/Al₂O₃-ZrO₂ Catalysts Prepared via a Direct Sol-Gel Process. *J. Nat. Gas Chem.* **2011**, *20*, 1–8. [[CrossRef](#)]
114. González, A.R.; Asencios, Y.J.O.; Assaf, E.M.; Assaf, J.M. Dry Reforming of Methane on Ni-Mg-Al Nano-Spheroid Oxide Catalysts Prepared by the Sol-Gel Method from Hydrotalcite-like Precursors. *Appl. Surf. Sci.* **2013**, *280*, 876–887. [[CrossRef](#)]
115. Salhi, N.; Boulahouache, A.; Petit, C.; Kiennemann, A.; Rabia, C. Steam Reforming of Methane to Syngas over NiAl₂O₄ Spinel Catalysts. *Int. J. Hydrogen Energy* **2011**, *36*, 11433–11439. [[CrossRef](#)]
116. Min, J.-E.; Lee, Y.-J.; Park, H.-G.; Zhang, C.; Jun, K.-W. Carbon Dioxide Reforming of Methane on Ni-MgO-Al₂O₃ Catalysts Prepared by Sol-Gel Method: Effects of Mg/Al Ratios. *J. Ind. Eng. Chem.* **2015**, *26*, 375–383. [[CrossRef](#)]
117. Sunde, T.O.L.; Grande, T.; Einarsrud, M.-A. Modified Pechini Synthesis of Oxide Powders and Thin Films. In *Handbook of Sol-Gel Science and Technology*; Klein, L., Aparicio, M., Jitianu, A., Eds.; Springer International Publishing: Cham, Switzerland, 2016; pp. 1–30.
118. Rivas, M.E.; Fierro, J.L.G.; Guil-López, R.; Peña, M.A.; La Parola, V.; Goldwasser, M.R. Preparation and Characterization of Nickel-Based Mixed-Oxides and Their Performance for Catalytic Methane Decomposition. *Catal. Today* **2008**, *133–135*, 367–373. [[CrossRef](#)]
119. Rogers, J.L.; Mangarella, M.C.; D’Amico, A.D.; Gallagher, J.R.; Dutzer, M.R.; Stavitski, E.; Miller, J.T.; Sievers, C. Differences in the Nature of Active Sites for Methane Dry Reforming and Methane Steam Reforming over Nickel Aluminate Catalysts. *ACS Catal.* **2016**, *6*, 5873–5886. [[CrossRef](#)]
120. Schimmoeller, B.; Pratsinis, S.E.; Baiker, A. Flame Aerosol Synthesis of Metal Oxide Catalysts with Unprecedented Structural and Catalytic Properties. *ChemCatChem* **2011**, *3*, 1234–1256. [[CrossRef](#)]
121. Suh, D.J.; Park, T.-J.; Kim, J.-H.; Kim, K.-L. Nickel-Alumina Aerogel Catalysts Prepared by Fast Sol-Gel Synthesis. *J. Non-Cryst. Solids* **1998**, *225*, 168–172. [[CrossRef](#)]
122. Sebai, I.; Boulahouache, A.; Trari, M.; Salhi, N. Preparation and Characterization of 5%Ni/γ-Al₂O₃ Catalysts by Complexation with NH₃ Derivatives Active in Methane Steam Reforming. *Int. J. Hydrogen Energy* **2019**, *44*, 9949–9958. [[CrossRef](#)]
123. George, S.M. Atomic Layer Deposition: An Overview. *Chem. Rev.* **2010**, *110*, 111–131. [[CrossRef](#)]
124. Shang, Z.; Li, S.; Li, L.; Liu, G.; Liang, X. Highly Active and Stable Alumina Supported Nickel Nanoparticle Catalysts for Dry Reforming of Methane. *Appl. Catal. B Environ.* **2017**, *201*, 302–309. [[CrossRef](#)]
125. Wang, G.; Luo, F.; Cao, K.; Zhang, Y.; Li, J.; Zhao, F.; Chen, R.; Hong, J. Effect of Ni Content of Ni/γ-Al₂O₃ Catalysts Prepared by the Atomic Layer Deposition Method on CO₂ Reforming of Methane. *Energy Technol.* **2019**, *7*, 1800359. [[CrossRef](#)]
126. Jeong, M.-G.; Kim, S.Y.; Kim, D.H.; Han, S.W.; Kim, I.H.; Lee, M.; Hwang, Y.K.; Kim, Y.D. High-Performing and Durable MgO/Ni Catalysts via Atomic Layer Deposition for CO₂ Reforming of Methane (CRM). *Appl. Catal. A Gen.* **2016**, *515*, 45–50. [[CrossRef](#)]
127. Gould, T.D.; Izar, A.; Weimer, A.W.; Falconer, J.L.; Medlin, J.W. Stabilizing Ni Catalysts by Molecular Layer Deposition for Harsh, Dry Reforming Conditions. *ACS Catal.* **2014**, *4*, 2714–2717. [[CrossRef](#)]
128. Littlewood, P.; Liu, S.; Weitz, E.; Marks, T.J.; Stair, P.C. Ni-Alumina Dry Reforming Catalysts: Atomic Layer Deposition and the Issue of Ni Aluminate. *Catal. Today* **2020**, *343*, 18–25. [[CrossRef](#)]
129. Kim, H.; Eissa, A.A.-S.; Kim, S.B.; Lee, H.; Kim, W.; Seo, D.J.; Lee, K.; Yoon, W.L. One-Pot Synthesis of a Highly Mesoporous Ni/MgAl₂O₄ Spinel Catalyst for Efficient Steam Methane Reforming: Influence of Inert Annealing. *Catal. Sci. Technol.* **2021**, *11*, 4447–4458. [[CrossRef](#)]
130. Guo, Y.; Li, Y.; Ning, Y.; Liu, Q.; Tian, L.; Zhang, R.; Fu, Q.; Wang, Z. CO₂ Reforming of Methane over a Highly Dispersed Ni/Mg-Al-O Catalyst Prepared by a Facile and Green Method. *Ind. Eng. Chem. Res.* **2020**, *59*, 15506–15514. [[CrossRef](#)]
131. Huang, J.; Yan, Y.; Saqline, S.; Liu, W.; Liu, B. High Performance Ni Catalysts Prepared by Freeze Drying for Efficient Dry Reforming of Methane. *Appl. Catal. B Environ.* **2020**, *275*, 119109. [[CrossRef](#)]
132. Kobayashi, N.; Takahashi, S. Catalyst for Decomposition of Hydrocarbons, Process for Producing the Catalyst, and Process for Producing Hydrogen Using the Catalyst. U.S. Patent 7196036B2, 27 March 2007.
133. Kwak, G.; Park, H.; Wi, S.; Park, S. High Efficiency Ni-based Catalyst for Steam Methane Reforming and Steam Methane Reforming Reaction using the Same. KR Patent 20220052099A, 27 April 2022.
134. Hou, Z.; Yashima, T. Small Amounts of Rh-Promoted Ni Catalysts for Methane Reforming with CO₂. *Catal. Lett.* **2003**, *89*, 193–197. [[CrossRef](#)]
135. Fei, J.; Hou, Z.; Zheng, X.; Yashima, T. Doped Ni Catalysts for Methane Reforming with CO₂. *Catal. Lett.* **2004**, *98*, 241–246. [[CrossRef](#)]
136. Crisafulli, C.; Scirè, S.; Minicò, S.; Solarino, L. Ni-Ru Bimetallic Catalysts for the CO₂ Reforming of Methane. *Appl. Catal. A Gen.* **2002**, *225*, 1–9. [[CrossRef](#)]
137. Tomishige, K.; Kanazawa, S.; Sato, M.; Ikushima, K.; Kunimori, K. Catalyst Design of Pt-Modified Ni/Al₂O₃ Catalyst with Flat Temperature Profile in Methane Reforming with CO₂ and O₂. *Catal. Lett.* **2002**, *84*, 69–74. [[CrossRef](#)]
138. Dias, J.A.C.; Assaf, J.M. Autothermal Reforming of Methane over Ni/γ-Al₂O₃ Catalysts: The Enhancement Effect of Small Quantities of Noble Metals. *J. Power Sources* **2004**, *130*, 106–110. [[CrossRef](#)]

139. Dias, J.A.C.; Assaf, J.M. Autoreduction of Promoted Ni/ γ -Al₂O₃ during Autothermal Reforming of Methane. *J. Power Sources* **2005**, *139*, 176–181. [CrossRef]
140. Daza, C.E.; Gallego, J.; Mondragón, F.; Moreno, S.; Molina, R. High Stability of Ce-Promoted Ni/Mg–Al Catalysts Derived from Hydrotalcites in Dry Reforming of Methane. *Fuel* **2010**, *89*, 592–603. [CrossRef]
141. Laosiripojana, N.; Sutthisripok, W.; Assabumrungrat, S. Synthesis Gas Production from Dry Reforming of Methane over CeO₂ Doped Ni/Al₂O₃: Influence of the Doping Ceria on the Resistance toward Carbon Formation. *Chem. Eng. J.* **2005**, *112*, 13–22. [CrossRef]
142. Abd Ghani, N.A.; Azapour, A.; Syed Muhammad, A.F.; Abdullah, B. Dry Reforming of Methane for Hydrogen Production over NiCo Catalysts: Effect of NbZr Promoters. *Int. J. Hydrogen Energy* **2019**, *44*, 20881–20888. [CrossRef]
143. Navarro, M.V.; Plou, J.; López, J.M.; Grasa, G.; Murillo, R. Effect of Oxidation-Reduction Cycles on Steam-Methane Reforming Kinetics over a Nickel-Based Catalyst. *Int. J. Hydrogen Energy* **2019**, *44*, 12617–12627. [CrossRef]
144. Álvarez, M.A.; Bobadilla, L.F.; Garcilaso, V.; Centeno, M.A.; Odriozola, J.A. CO₂ Reforming of Methane over Ni-Ru Supported Catalysts: On the Nature of Active Sites by Operando DRIFTS Study. *J. CO₂ Util.* **2018**, *24*, 509–515. [CrossRef]
145. Foletto, E.L.; Alves, R.W.; Jahn, S.L. Preparation of Ni/Pt Catalysts Supported on Spinel (MgAl₂O₄) for Methane Reforming. *J. Power Sources* **2006**, *161*, 531–534. [CrossRef]
146. Jaiswar, V.K.; Katheria, S.; Deo, G.; Kunzru, D. Effect of Pt Doping on Activity and Stability of Ni/MgAl₂O₄ Catalyst for Steam Reforming of Methane at Ambient and High Pressure Condition. *Int. J. Hydrogen Energy* **2017**, *42*, 18968–18976. [CrossRef]
147. Yoshida, K.; Begum, N.; Ito, S.; Tomishige, K. Oxidative Steam Reforming of Methane over Ni/ α -Al₂O₃ Modified with Trace Noble Metals. *Appl. Catal. A Gen.* **2009**, *358*, 186–192. [CrossRef]
148. Li, B.; Kado, S.; Mukainakano, Y.; Miyazawa, T.; Miyao, T.; Naito, S.; Okumura, K.; Kunimori, K.; Tomishige, K. Surface Modification of Ni Catalysts with Trace Pt for Oxidative Steam Reforming of Methane. *J. Catal.* **2007**, *245*, 144–155. [CrossRef]
149. Arena, F.; Horrell, B.A.; Cocke, D.L.; Parmaliana, A.; Giordano, N. Magnesia-Supported Nickel Catalysts I. Factors Affecting the Structure and Morphological Properties. *J. Catal.* **1991**, *132*, 58–67. [CrossRef]
150. Nurunnabi, M.; Mukainakano, Y.; Kado, S.; Miyazawa, T.; Okumura, K.; Miyao, T.; Naito, S.; Suzuki, K.; Fujimoto, K.-I.; Kunimori, K.; et al. Oxidative Steam Reforming of Methane under Atmospheric and Pressurized Conditions over Pd/NiO–MgO Solid Solution Catalysts. *Appl. Catal. A Gen.* **2006**, *308*, 1–12. [CrossRef]
151. Katheria, S.; Deo, G.; Kunzru, D. Rh-Ni/MgAl₂O₄ Catalyst for Steam Reforming of Methane: Effect of Rh Doping, Calcination Temperature and Its Application on Metal Monoliths. *Appl. Catal. A Gen.* **2019**, *570*, 308–318. [CrossRef]
152. Prins, R. Hydrogen Spillover. Facts and Fiction. *Chem. Rev.* **2012**, *112*, 2714–2738. [CrossRef] [PubMed]
153. Takehira, K. “Intelligent” Reforming Catalysts: Trace Noble Metal-Doped Ni/Mg(Al)O Derived from Hydrotalcites. *J. Nat. Gas Chem.* **2009**, *18*, 237–259. [CrossRef]
154. Li, D.; Zhan, Y.; Nishida, K.; Oumi, Y.; Sano, T.; Shishido, T.; Takehira, K. “Green” Preparation of “Intelligent” Pt-Doped Ni/Mg(Al)O Catalysts for Daily Start-up and Shut-down CH₄ Steam Reforming. *Appl. Catal. A Gen.* **2009**, *363*, 169–179. [CrossRef]
155. Miyata, T.; Li, D.; Shiraga, M.; Shishido, T.; Oumi, Y.; Sano, T.; Takehira, K. Promoting Effect of Rh, Pd and Pt Noble Metals to the Ni/Mg(Al)O Catalysts for the DSS-like Operation in CH₄ Steam Reforming. *Appl. Catal. A Gen.* **2006**, *310*, 97–104. [CrossRef]
156. Katheria, S.; Kunzru, D.; Deo, G. Kinetics of Steam Reforming of Methane on Rh–Ni/MgAl₂O₄ Catalyst. *React. Kinet. Mech. Catal.* **2020**, *130*, 91–101. [CrossRef]
157. Jeong, J.H.; Lee, J.W.; Seo, D.J.; Seo, Y.; Yoon, W.L.; Lee, D.K.; Kim, D.H. Ru-Doped Ni Catalysts Effective for the Steam Reforming of Methane without the Pre-Reduction Treatment with H₂. *Appl. Catal. A Gen.* **2006**, *302*, 151–156. [CrossRef]
158. Baek, S.-C.; Jun, K.-W.; Lee, Y.-J.; Kim, J.D.; Park, D.Y.; Lee, K.-Y. Ru/Ni/MgAl₂O₄ Catalysts for Steam Reforming of Methane: Effects of Ru Content on Self-Activation Property. *Res. Chem. Intermed.* **2012**, *38*, 1225–1236. [CrossRef]
159. Nawfal, M.; Gennequin, C.; Labaki, M.; Nsouli, B.; Aboukais, A.; Abi-Aad, E. Hydrogen Production by Methane Steam Reforming over Ru Supported on Ni–Mg–Al Mixed Oxides Prepared via Hydrotalcite Route. *Int. J. Hydrogen Energy* **2015**, *40*, 1269–1277. [CrossRef]
160. Kim, N.Y.; Yang, E.-H.; Lim, S.-S.; Jung, J.S.; Lee, J.-S.; Hong, G.H.; Noh, Y.-S.; Lee, K.Y.; Moon, D.J. Hydrogen Production by Steam Reforming of Methane over Mixed Ni/MgAl + CrFe₃O₄ Catalysts. *Int. J. Hydrogen Energy* **2015**, *40*, 11848–11854. [CrossRef]
161. Kim, D.H.; Youn, J.-R.; Seo, J.-C.; Kim, S.B.; Kim, M.-J.; Lee, K. One-Pot Synthesis of NiCo/MgAl₂O₄ Catalyst for High Coke-Resistance in Steam Methane Reforming: Optimization of Ni/Co Ratio. *Catal. Today* **2022**, in press. [CrossRef]
162. Bossola, F.; Roongcharoen, T.; Coduri, M.; Evangelisti, C.; Somodi, F.; Sementa, L.; Fortunelli, A.; Dal Santo, V. Discovering Indium as Hydrogen Production Booster for a Cu/SiO₂ Catalyst in Steam Reforming of Methanol. *Appl. Catal. B Environ.* **2021**, *297*, 120398. [CrossRef]
163. Etmnan, A.; Sadrnezhad, S.K. A Two Step Microwave-Assisted Coke Resistant Mesoporous Ni-Co Catalyst for Methane Steam Reforming. *Fuel* **2022**, *317*, 122411. [CrossRef]
164. Moon, D.J.; Lee, Y.J.; Jung, J.S.; Lee, J.H.; Lee, S.H.; Kim, B.H.; Kim, H.J.; Yang, E.H. Alkaline Earth Metal Co-Precipitated Nickel-Based Catalyst for Steam Carbon Dioxide Reforming of Natural Gas. US Patent 20140339475A, 3 March 2015.
165. Du, J.; Liu, P.; Gao, Z.; Zhang, W.; Zhang, L.; Li, X. Magnesium Aluminate Spinel Type Composite Oxide Carrier, Preparation Method Thereof and Steam Reforming Catalyst. CN Patent 112844388A, 29 November 2022.
166. Chin, Y.-H.; King, D.L.; Roh, H.-S.; Wang, Y.; Heald, S.M. Structure and Reactivity Investigations on Supported Bimetallic AuNi Catalysts Used for Hydrocarbon Steam Reforming. *J. Catal.* **2006**, *244*, 153–162. [CrossRef]
167. *Binary Alloy Phase Diagrams*, 2nd ed; Massalski, T.B.; Okamoto, H.; Subramanian, P.R.; Kacprzak, L. (Eds.) ASM International: Materials Park, OH, USA, 1990.

168. Bengaard, H.S.; Nørskov, J.K.; Sehested, J.; Clausen, B.S.; Nielsen, L.P.; Molenbroek, A.M.; Rostrup-Nielsen, J.R. Steam Reforming and Graphite Formation on Ni Catalysts. *J. Catal.* **2002**, *209*, 365–384. [[CrossRef](#)]
169. Zhan, Y.; Li, D.; Nishida, K.; Shishido, T.; Oumi, Y.; Sano, T.; Takehira, K. Preparation of “Intelligent” Pt/Ni/Mg(Al)O Catalysts Starting from Commercial Mg–Al LDHs for Daily Start-up and Shut-down Steam Reforming of Methane. *Appl. Clay Sci.* **2009**, *45*, 147–154. [[CrossRef](#)]
170. Ko, J.; Kim, B.-K.; Han, J.W. Density Functional Theory Study for Catalytic Activation and Dissociation of CO₂ on Bimetallic Alloy Surfaces. *J. Phys. Chem. C* **2016**, *120*, 3438–3447. [[CrossRef](#)]
171. Zhang, J.; Wang, H.; Dalai, A.K. Effects of Metal Content on Activity and Stability of Ni–Co Bimetallic Catalysts for CO₂ Reforming of CH₄. *Appl. Catal. A Gen.* **2008**, *339*, 121–129. [[CrossRef](#)]
172. Niu, J.; Wang, Y.; Liland, E.S.; Regli, K.S.; Yang, J.; Rout, K.R.; Luo, J.; Rønning, M.; Ran, J.; Chen, D. Unraveling Enhanced Activity, Selectivity, and Coke Resistance of Pt–Ni Bimetallic Clusters in Dry Reforming. *ACS Catal.* **2021**, *11*, 2398–2411. [[CrossRef](#)]
173. Álvarez Moreno, A.; Ramirez-Reina, T.; Ivanova, S.; Roger, A.-C.; Centeno, M.Á.; Odriozola, J.A. Bimetallic Ni–Ru and Ni–Re Catalysts for Dry Reforming of Methane: Understanding the Synergies of the Selected Promoters. *Front. Chem.* **2021**, *9*, 694976. [[CrossRef](#)] [[PubMed](#)]
174. Bian, Z.; Das, S.; Wai, M.H.; Hongmanorom, P.; Kawi, S. A Review on Bimetallic Nickel-Based Catalysts for CO₂ Reforming of Methane. *ChemPhysChem* **2017**, *18*, 3117–3134. [[CrossRef](#)] [[PubMed](#)]
175. Ferreira-Aparicio, P.; Fernandez-Garcia, M.; Guerrero-Ruiz, A.; Rodriguez-Ramos, I. Evaluation of the Role of the Metal–Support Interfacial Centers in the Dry Reforming of Methane on Alumina-Supported Rhodium Catalysts. *J. Catal.* **2000**, *190*, 296–308. [[CrossRef](#)]
176. Nematollahi, B.; Rezaei, M.; Khajenoori, M. Combined Dry Reforming and Partial Oxidation of Methane to Synthesis Gas on Noble Metal Catalysts. *Int. J. Hydrogen Energy* **2011**, *36*, 2969–2978. [[CrossRef](#)]
177. Wang, H.Y.; Au, C.T. Carbon Dioxide Reforming of Methane to Syngas over SiO₂-Supported Rhodium Catalysts. *Appl. Catal. A Gen.* **1997**, *155*, 239–252. [[CrossRef](#)]
178. Wu, H.; Pantaleo, G.; La Parola, V.; Venezia, A.M.; Collard, X.; Aprile, C.; Liotta, L.F. Bi- and Trimetallic Ni Catalysts over Al₂O₃ and Al₂O₃-MO_x (M=Ce or Mg) Oxides for Methane Dry Reforming: Au and Pt Additive Effects. *Appl. Catal. B Environ.* **2014**, *156–157*, 350–361. [[CrossRef](#)]
179. Yu, X.; Zhang, F.; Wang, N.; Hao, S.; Chu, W. Plasma-Treated Bimetallic Ni–Pt Catalysts Derived from Hydrotalcites for the Carbon Dioxide Reforming of Methane. *Catal. Lett.* **2014**, *144*, 293–300. [[CrossRef](#)]
180. Osaki, T.; Mori, T. Role of Potassium in Carbon-Free CO₂ Reforming of Methane on K-Promoted Ni/Al₂O₃ Catalysts. *J. Catal.* **2001**, *204*, 89–97. [[CrossRef](#)]
181. García-Diéguez, M.; Pieta, I.S.; Herrera, M.C.; Larrubia, M.A.; Alemany, L.J. Nanostructured Pt- and Ni-Based Catalysts for CO₂-Reforming of Methane. *J. Catal.* **2010**, *270*, 136–145. [[CrossRef](#)]
182. Li, L.; Anjum, D.H.; Zhu, H.; Saih, Y.; Laveille, P.V.; D’Souza, L.; Basset, J.-M. Synergetic Effects Leading to Coke-Resistant NiCo Bimetallic Catalysts for Dry Reforming of Methane. *ChemCatChem* **2015**, *7*, 427–433. [[CrossRef](#)]
183. Hu, Y.H. Solid-Solution Catalysts for CO₂ Reforming of Methane. *Catal. Today* **2009**, *148*, 206–211. [[CrossRef](#)]
184. Duan, X.; Pan, J.; Yang, X.; Wan, C.; Lin, X.; Li, D.; Jiang, L. Nickel-cobalt Bimetallic Catalysts Prepared from Hydrotalcite-like Compounds for Dry Reforming of Methane. *Int. J. Hydrogen Energy* **2022**, *47*, 24358–24373. [[CrossRef](#)]
185. Torimoto, M.; Sekine, Y. Effects of Alloying for Steam or Dry Reforming of Methane: A Review of Recent Studies. *Catal. Sci. Technol.* **2022**, *12*, 3387–3411. [[CrossRef](#)]
186. Tsyganok, A.I.; Inaba, M.; Tsunoda, T.; Uchida, K.; Suzuki, K.; Takehira, K.; Hayakawa, T. Rational Design of Mg–Al Mixed Oxide-Supported Bimetallic Catalysts for Dry Reforming of Methane. *Appl. Catal. A Gen.* **2005**, *292*, 328–343. [[CrossRef](#)]
187. Miyata, S. Physico-Chemical Properties of Synthetic Hydrotalcites in Relation to Composition. *Clays Clay Miner.* **1980**, *28*, 50–56. [[CrossRef](#)]
188. Tsyganok, A.I.; Inaba, M.; Tsunoda, T.; Suzuki, K.; Takehira, K.; Hayakawa, T. Combined Partial Oxidation and Dry Reforming of Methane to Synthesis Gas over Noble Metals Supported on Mg–Al Mixed Oxide. *Appl. Catal. A Gen.* **2004**, *275*, 149–155. [[CrossRef](#)]
189. Wysocka, I.; Hupka, J.; Rogala, A. Catalytic Activity of Nickel and Ruthenium–Nickel Catalysts Supported on SiO₂, ZrO₂, Al₂O₃, and MgAl₂O₄ in a Dry Reforming Process. *Catalysts* **2019**, *9*, 540. [[CrossRef](#)]
190. Lucrédio, A.F.; Assaf, J.M.; Assaf, E.M. Methane Conversion Reactions on Ni Catalysts Promoted with Rh: Influence of Support. *Appl. Catal. A Gen.* **2011**, *400*, 156–165. [[CrossRef](#)]
191. Theofanidis, S.A.; Galvita, V.V.; Poelman, H.; Marin, G.B. Enhanced Carbon-Resistant Dry Reforming Fe–Ni Catalyst: Role of Fe. *ACS Catal.* **2015**, *5*, 3028–3039. [[CrossRef](#)]
192. Theofanidis, S.A.; Batchu, R.; Galvita, V.V.; Poelman, H.; Marin, G.B. Carbon Gasification from Fe–Ni Catalysts after Methane Dry Reforming. *Appl. Catal. B Environ.* **2016**, *185*, 42–55. [[CrossRef](#)]
193. Wan, C.; Song, K.; Pan, J.; Huang, M.; Luo, R.; Li, D.; Jiang, L. Ni–Fe/Mg(Al)O Alloy Catalyst for Carbon Dioxide Reforming of Methane: Influence of Reduction Temperature and Ni–Fe Alloying on Coking. *Int. J. Hydrogen Energy* **2020**, *45*, 33574–33585. [[CrossRef](#)]
194. Wang, L.; Li, D.; Koike, M.; Koso, S.; Nakagawa, Y.; Xu, Y.; Tomishige, K. Catalytic Performance and Characterization of Ni–Fe Catalysts for the Steam Reforming of Tar from Biomass Pyrolysis to Synthesis Gas. *Appl. Catal. A Gen.* **2011**, *392*, 248–255. [[CrossRef](#)]

195. Ray, K.; Sengupta, S.; Deo, G. Reforming and Cracking of CH₄ over Al₂O₃ Supported Ni, Ni-Fe and Ni-Co Catalysts. *Fuel Process. Technol.* **2017**, *156*, 195–203. [[CrossRef](#)]
196. Boudjeloud, M.; Boulahouache, A.; Rabia, C.; Salhi, N. La-Doped Supported Ni Catalysts for Steam Reforming of Methane. *Int. J. Hydrogen Energy* **2019**, *44*, 9906–9913. [[CrossRef](#)]
197. Ohi, T.; Miyata, T.; Li, D.; Shishido, T.; Kawabata, T.; Sano, T.; Takehira, K. Sustainability of Ni Loaded Mg–Al Mixed Oxide Catalyst in Daily Startup and Shutdown Operations of CH₄ Steam Reforming. *Appl. Catal. A Gen.* **2006**, *308*, 194–203. [[CrossRef](#)]
198. Benito, P.; Dal Santo, V.; De Grandi, V.; Marelli, M.; Fornasari, G.; Psaro, R.; Vaccari, A. Coprecipitation versus Chemical Vapour Deposition to Prepare Rh/Ni Bimetallic Catalysts. *Appl. Catal. B Environ.* **2015**, *179*, 150–159. [[CrossRef](#)]
199. Huang, Y.; Du, J.; Ling, C.; Zhou, T.; Wang, S. Methane Dehydrogenation on Au/Ni Surface Alloys—A First-Principles Study. *Catal. Sci. Technol.* **2013**, *3*, 1343–1354. [[CrossRef](#)]
200. Niu, J.; Wang, Y.; Qi, Y.; Dam, A.H.; Wang, H.; Zhu, Y.-A.; Holmen, A.; Ran, J.; Chen, D. New Mechanism Insights into Methane Steam Reforming on Pt/Ni from DFT and Experimental Kinetic Study. *Fuel* **2020**, *266*, 117143. [[CrossRef](#)]
201. De Coster, V.; Srinath, N.V.; Theofanidis, S.A.; Pirro, L.; Van Alboom, A.; Poelman, H.; Sabbe, M.K.; Marin, G.B.; Galvita, V.V. Looking inside a Ni-Fe/MgAl₂O₄ Catalyst for Methane Dry Reforming via Mössbauer Spectroscopy and in Situ QXAS. *Appl. Catal. B Environ.* **2022**, *300*, 120720. [[CrossRef](#)]
202. Meloni, E.; Martino, M.; Palma, V. A Short Review on Ni Based Catalysts and Related Engineering Issues for Methane Steam Reforming. *Catalysts* **2020**, *10*, 352. [[CrossRef](#)]

Disclaimer/Publisher’s Note: The statements, opinions and data contained in all publications are solely those of the individual author(s) and contributor(s) and not of MDPI and/or the editor(s). MDPI and/or the editor(s) disclaim responsibility for any injury to people or property resulting from any ideas, methods, instructions or products referred to in the content.